Spiniferites cruciformis, Pterocysta cruciformis and Galeacysta etrusca

morphology and palaeoecology

Mudie, P.; Rochon, A.; Richards, K.; Ferguson, S.; Warny, S.

DOI
10.1080/01916122.2018.1465737

Publication date
2018

Document Version
Final published version

Published in
Palynology

PALYNOLOGY
2018, VOL. 42, NO. S1, 135–161
https://doi.org/10.1080/01916122.2018.1465737

Spiniferites cruciformis, *Pterocysta cruciformis* and *Galeacysta etrusca*: morphology and palaeoecology

Peta Mudie[a], André Rochon[b], Keith Richards[c,d], Shannon Ferguson[e] and Sophie Warny[e]

[a]Geological Survey Canada-Atlantic, Dartmouth, Canada; [b]ISMER, Université du Québec à Rimouski, Rimouski, Canada; [c]KrA Stratigraphic Ltd., Conwy, UK; [d]Institute for Biodiversity and Ecosystem Dynamics (IBED), University of Amsterdam, Amsterdam, The Netherlands; [e]Department of Geology and Geophysics, and Museum of Natural Science, Louisiana State University, Baton Rouge, LA, USA

ABSTRACT

Miocene to modern sediments of the Ponto-Caspian basins and Mediterranean Sea are uniquely distinguished by presence of gonyaulacacean cysts with ellipsoid to cruciform endocysts and highly variable ectocystal features, including pterate (wing-like) and galeate (helmet-like) outer wall layers. The term cruciform is defined to indicate cysts with concave epicyst and hypocyst surfaces and moderate dorsoventral flattening. These features may be morphological responses to salinity stress and some biometrical studies conclude that the cruciform Ponto-Caspian species *Spiniferites cruciformis* of Wall and Dale 1973 and *Pterocysta cruciformis* Rochon et al. 2003 are morphotypes of the ellipsoidal-subpentagonal Miocene-Holocene species *Galeacysta etrusca* Corradini and Biffi 1988. We show that the holotypes of these cruciform and rhomboid-subpentagonal galeate taxa differ in endocyst shape, ectocyst structure and attachment points, process morphology, and sulcal plate expression, and we present new data on morphological variations, modern distribution and ecology. We list multiple criteria for distinguishing these taxa from Paratethyan dinoflagellates with shared features, including *Thalassiphora* spp., *Lophocysta, Romanodinium,* and *Seriliodinium*. Log transforms of endocyst:ectocyst (EN:EC) dimensions cannot fully capture cruciformness or galeate and pterate wall characteristics that distinguish the genera, and at DSDP Site 380, EN:EC values for Pleistocene populations of *Spiniferites cruciformis* and *Galeacysta etrusca* are significantly different. Re-examination of the history of studies on the *Galeacysta etrusca* complex and comparison with new studies of Pleistocene to recent cysts leads to the conclusion there is insufficient evidence to justify combining the cruciform species with *Galeacysta etrusca* and we provide criteria for distinguishing among the main components of the complex. Using multiple morphological features, it appears there is a replacement of large Palaeogene marine-brackish water camocavate-circumcavate taxa with elliptical endocysts first by the Miocene rhombo-subpentagonal galeate species *Galeacysta etrusca* and then by the Pliocene – Holocene semi-marine–brackish cruciform species *Spiniferites cruciformis* and stenohaline *Pterocysta cruciformis*.

KEYWORDS
Cruciform cyst; chronostratigraphy; palaeosalinity; Paratethys; Ponto-Caspian

1. Introduction

Spiniferites cruciformis Wall & Dale in Wall et al. 1973, *Pterocysta cruciformis* Rochon et al. 2003 and *Galeacysta etrusca* Corradini and Biffi (1988) are three species of gonyaulacacean dinoflagellate cysts (dinocysts) which occur exclusively in the Paratethyan and Ponto-Caspian regions and in northern Mediterranean marine to lacustrine basins, from Miocene to modern time. Notably, these species are not found at Mio-Pliocene sites in the southwestern Mediterranean Sea, at the connection between the Alboran Sea and the Miocene Rifian and Betic palaeostraits (Warny and Wrenn 1997, 2002; Warny et al. 2003) or in the Atlantic Ocean west of the Iberian Abyssal Plain. The Ponto-Caspian and Paratethyan taxa are characterised by either a cruciform or sub-pentagonal endocyst shape and by highly variable development of septa and ectophragms (Figure 1). The extinct Plio-Pleistocene species *Seriliodinium explicatum* Eaton 1996 also has a cruciform endocyst shape and may be a trabeculate morphotype of *Spiniferites cruciformis* (see Sect. 2.2).

The distinctive cruciform endocyst shape and highly variable development of processes and parasutural septa of the Ponto-Caspian – Mediterranean cruciform taxa are important features because they have been interpreted as reflecting morphological responses to salinity stress (Wall et al. 1973; Dale 1996; Ellegaard 2000; Mudie et al. 2001). According to Londeix et al. (2007), few dinocyst taxa are strictly indicative of low salinity and these are often endemic to isolated basins where they are frequently characterised by elaborate ornamentation as seen in *Spiniferites cruciformis*, *Pterocysta cruciformis*, *Seriliodinium explicatum* and *Galeacysta etrusca*. Consequently, these taxa have been widely used as proxies for surface water salinity, sea level change, and marine-lacustrine linkages (e.g. Londeix et al. 2007; Popescu et al. 2007; Bakrač et al. 2012; Suc et al. 2015; Grothe et al. 2014), despite the lack of well-constrained data for their ecological distribution and salinity tolerance which we aim to address in this paper. The salinity terms we use are those employed for studies of basins in the Ponto-Caspian region which includes the Black Sea and Sea of Azov (a.k.a. the Pontic

CONTACT Peta Mudie mudiep@ns.sympatico.ca Geological Survey Canada-Atlantic, Dartmouth, Canada

Published online 14 Dec 2018

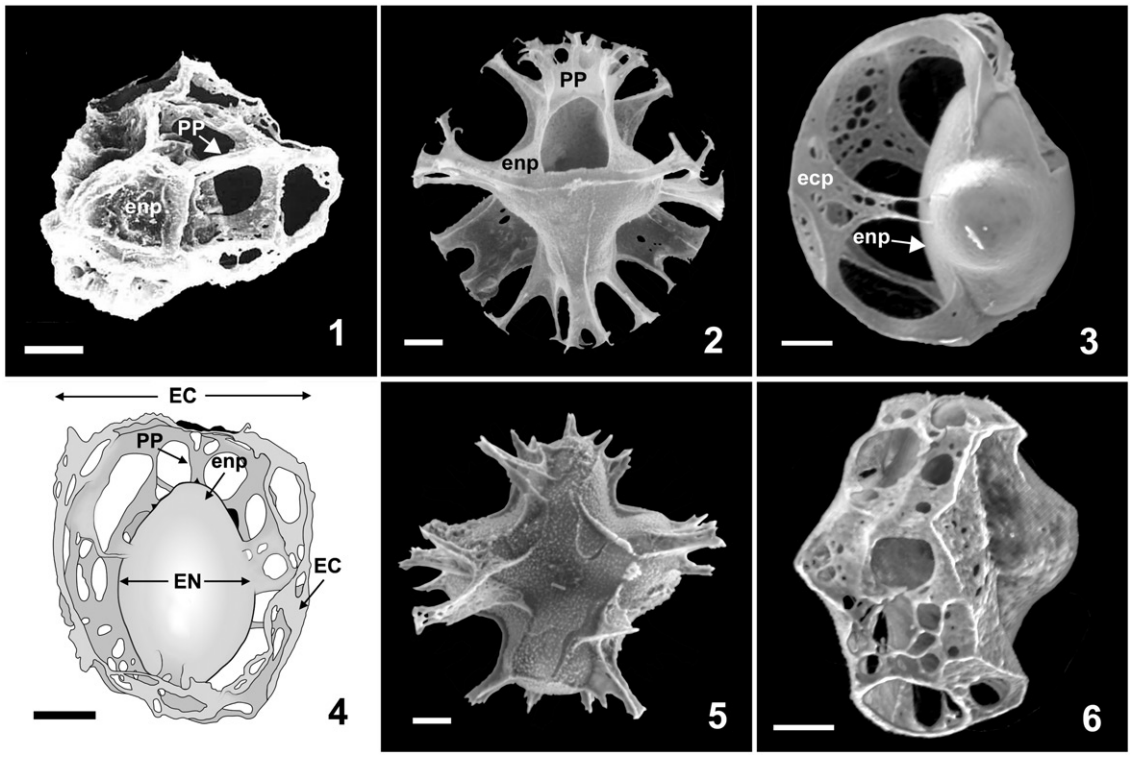

Figure 1. Equatorial views of dorsal (top) and ventral (bottom) surfaces of galeate, cruciform and pterate cyst species in the *Galeacysta etrusca* complex of Popescu et al. (2009), indicating cyst and wall layer terminology. Figures 1.1 and 1.4: *Galeacysta etrusca*. 1.1 oblique dorsal view of holotype, showing apical attachment points of the galeate periphragm (from Corradini and Biffi 1988); 1.4: ventral surface showing laterally enveloping galeate periphragm (line drawing by AR compiled using LM images of specimens from the Maccarone Lago Mare type locality). Figures 1.2, 1.5: *Spiniferites cruciformis* Black Sea paratype. 1.2 Dorsal view; 1.5 Ventral surface. Figures 1.3, 1.6: *Pterocysta cruciformis* topotype. 1.3 dorso-lateral view showing attachment of the narrow pterate ectophragm; 1.6 oblique view of ventral surface showing the diagnostic pterate 'wing' ectophragm and the dorso-ventrally compressed cyst body. EC = ectocyst, EN = endocyst, ecp = ectophragm, enp = endophragm, pp = periphragm. Scale bar = 20 μm for 1.1 and 1.4, 10 μm for the other images.

Seas), the Caspian Sea, and the Marmara Sea that links these interior seas to the easternmost Mediterranean region (Figure 2). Figure 2B also shows the general outline of the Central – Eastern Paratethyan Sea and the approximate locations of the Pliocene Pannonian, Dacian and Kracić lacustrine basins that were formerly linked to the Ponto-Caspian region basins and to the Mediterranean Sea. Details of smaller Paratethyan basins and the dynamics of their gateway locations and closures, however, must be sought elsewhere (e.g. Snel et al. 2006; Matenco et al. 2016).

Because of the wide range of endocyst shape and degree of outer wall development found in cruciform and galeate cysts from Holocene and older sediments, there have been several efforts to delimit morphotypes that correspond to different levels of basin salinity (Mudie et al. 2001; Marret et al. 2004; Popescu et al. 2009; Ferguson 2012). In particular, the large-scale (1100 specimens) biometrical studies of Popescu et al. (2009) used various ratios of endocyst to ectocyst dimensions to determine that the Pliocene – Recent species *Spiniferites cruciformis* and the Pleistocene species *Pterocysta cruciformis* which have cruciform endocysts are morphotypes of the Miocene–Pleistocene species *Galeacysta etrusca* which has an ellipsoidal to subpentagonal endocyst. There has also been a tendency for palynologists to group together diverse other Paratethyan and Ponto-Caspian genera that vary greatly in the morphological characteristics and to use this grouping in 'synthetic' palaeoenvironmental diagrams as all or part of 'brackish Paratethyan taxa' (Londeix et al. 2007; Popescu et al. 2007, 2015). Unfortunately, as a result of this grouping, individual species-environment relationships are often lost, and it is also not possible to determine the age-ranges of individual taxa within a synthetic group.

The primary objective of this paper is to review the taxonomy of the Ponto-Caspian and Paratethyan cruciform cyst-complex, starting with the first use of the term cruciform in 1973 to describe the cross-shaped endocyst (= central body) shape of *Spiniferites cruciformis* (Wall et al. 1973). We will show how this precise term gradually has been broadened to include rhombiform-subpentagonal, elliptical and other endocyst and outer body shapes so that its original meaning is in danger of being lost, at the cost of accuracy in identification and determination of the salinity and age ranges of cruciform and other Paratethyan taxa. We also summarise new data from both modern (surface, <500 cal yr) and older Holocene samples which allow us to assign quantitative salinity and temperature ranges to the extant taxa in the Ponto-Caspian Seas where salinity varies from freshwater to semi-marine, as shown in Figure 2. We examine the history of other species in the '*Galeacysta etrusca* complex' of Popescu et al. (2009) that occur primarily in the Pannonian–Dacic basins (Figure 2) and we provide a table for distinguishing among the taxa by key morphological features. We investigate problems in using log transforms of endocyst:ectocyst (EN:EC) dimensions to capture cruciformness (endocyst shape), ectophragm attachment positions and other key features that distinguish among the genera, and

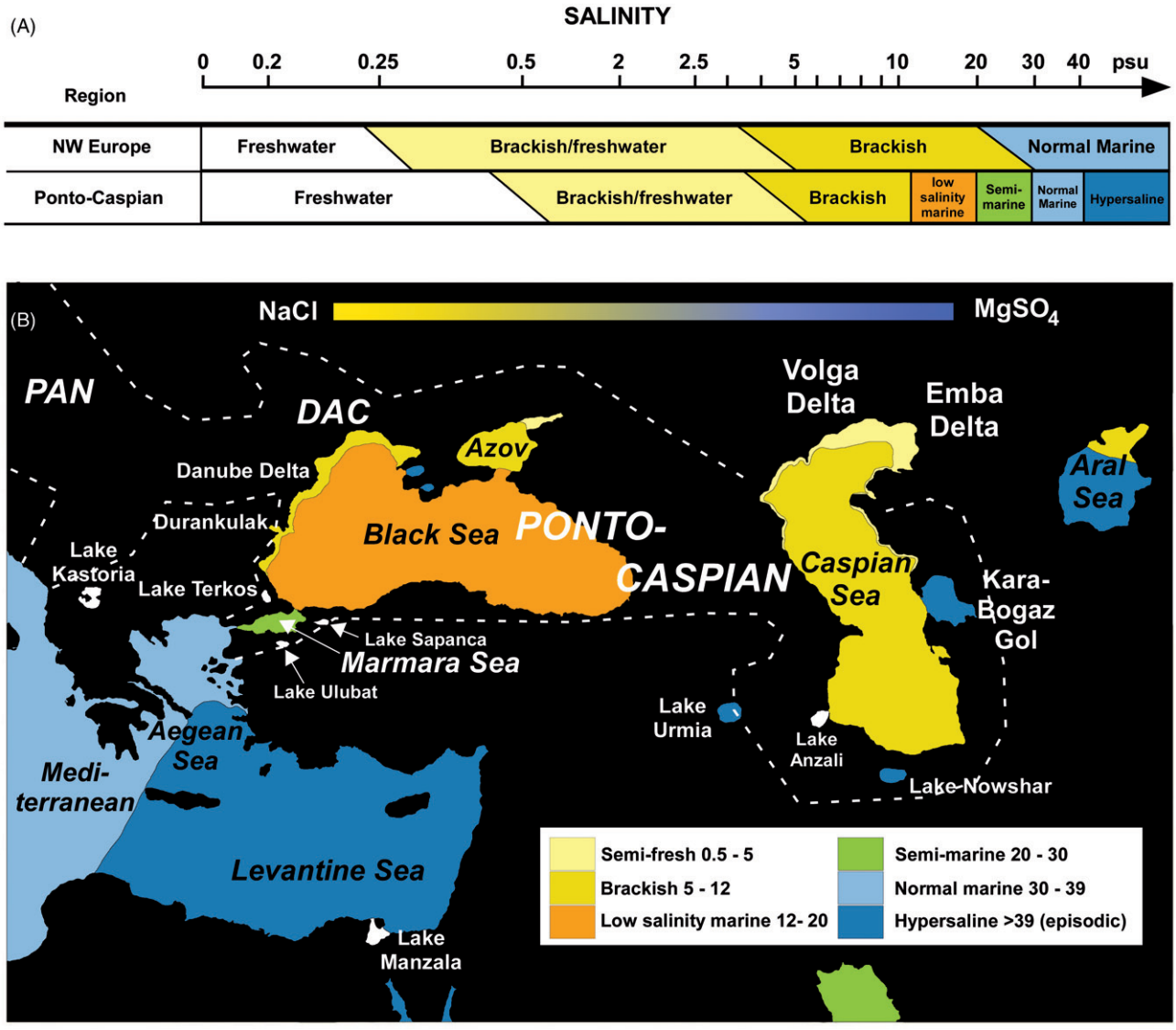

Figure 2. Salinity terminology (A) and location map (B) for the Ponto-Caspian region and adjacent Mediterranean region, showing places mentioned in the text and salinity terminology used in palaeoecological studies of planktonic microfossils in the study area and northwestern Europe (adapted from Mudie et al. 2011). Dashed lines delimit the general area covered by the Paratethyan Sea. PAN = Pannonian; DAC = Dacic; PONTO-CASPIAN = Pontic (= Black + Azov Seas) and Caspian Sea basins. The coloured bar at the top of (B) depicts the gradient of salt composition in the basins, from normal marine dominance of NaCl to prevalence of $MgSO_4$ and other salts in the endorheic continental basins of the Caspian and Aral Seas.

we show that reliance on EN:EC or other ratios rather than the full spectrum of cyst characteristics can lead to cyst misidentification and blurring of palaeosalinity signals. We provide criteria to distinguish among the components of the '*Galeacysta etrusca* complex' and show that this approach reveals a gradual replacement of the Miocene marine-brackish water rhombo-pentagonal galeate species *Galeocysta etrusca* by the Pliocene – Holocene fresh-brackish water cruciform to spindle-shaped, wide-crested or pterate (wing-bearing) species *Spiniferites cruciformis* and *Pterocysta cruciformis*.

2. History of cruciform and galeate cyst descriptions

In this section, we first provide definitions of terms that distinguish key species of the '*Galeacysta etrusca* complex' and in historical order, we highlight the salient features of the type species (readers can refer to the literature for the full original descriptions) and we add new information from our own research and recent literature. Generally, we do not give details of cyst morphology dimensions because these are tabulated in Section 3 where endocyst and ectocyst dimensions are compared. Because of the precedent established by Popescu et al. (2009), the terms endocyst (EN) and ectocyst (EC) are retained for the inner cyst body and extreme outer cyst body respectively, as used by Evitt et al. (1978), although the terms autocyst and pericyst might be used for *Spiniferites cruciformis*. The cyst wall layer terminology we employ (endophragm = enp, periphragm = pp, and ectophragm = ecp) is based on Evitt (1985, Figures 3.1F, 4.1E and J) and is shown in Figure 1. It relies on the observation that most *Spiniferites cruciformis* morphotypes show a small cavity (= pericoel) between the outer wall of the endocyst and some gonal process shafts, and traces of an outer wall layer occasionally are indicated by trabeculae joining the process tips. In *Pterocysta* a narrow fenestrate ectophragm is

attached by slender rods or broad septa. *Galeacysta* has a perforate outer wall attached by hollow processes.

2.1. Definitions of diagnostic characteristics

Regardless of the importance of the '*Galeacysta etrusca* complex' as a proxy for salinity, hitherto there have been no formal definitions of the terms cruciform, galeate and pterate in the context of dinocyst morphology, despite the widespread use of these adjectives in describing diagnostic endocyst shape and ectocyst characteristics for Paratethyan brackish-water marker species. The terms are therefore defined here in the following subsections.

2.1.1. Cruciform

The adjective 'cruciform' is not listed in the Williams et al. (2000) glossary of cyst morphology although it was introduced in 1973 to describe the endocyst of *Spiniferites cruciformis* in late Pleistocene-Holocene sediments (Wall et al. 1973). In the following year, it was used for the cyst outline of a new *Wetzeliella* species by Sarjeant (1974, p. 114). Later, Riding et al. (2000, p. 31) further used the adjective cruciform to describe the angular exocyst outline of the dorsoventrally-compressed, cornucavate species *Muderongia tomaszowensis* Albert 1961 which has a rounded-rectangular to subpentagonal endocyst. It is important to note, however, that the term was introduced by Barrie Dale (in Wall et al. 1973) to describe the distinctive shape of the **endocyst** (their test/cyst body) of *Spiniferites cruciformis* from late Pleistocene to early Holocene sediments of deep water sites in the Black Sea (Plates 1 and 2, Figures 1.2, 1.5). The outline (ambitus) of this chorate/proximochorate cyst is variable (see Sect. 2.2) but it is not cruciform except in rare proximate morphotypes (Form 5 of Mudie et al. 2002) where processes are absent and sutural septa are weakly developed.

Dictionaries define the adjective 'cruciform' as being in the shape of a cross (from Latin *crux* = cross and *-iform*), and it refers to the shape of a religious crucifix as opposed to an X-shaped cross. Following Wall et al. (1973), we define the cruciform cyst shape as indicating strongly concave precingular and postcingular lateral endocyst surfaces accompanied by moderate dorsoventral compression, giving the endocyst a cross-shaped appearance in equatorial view, a flattened ovoid to sub-rectangular appearance in polar view, and an almost rectangular shape in lateral view. The ratio of equatorial width to dorso-ventral thickness is cited as ca.1.4:1, i.e. the endocyst is almost 50% wider in the equatorial region than its thickness from dorsal to ventral surface.

Eaton (1996) later introduced the adjective subcruciform to describe the 'rounded cruciform' shape of the endocyst in a *Thalassiphora*-like taxon from a Black Sea dredge sample containing specimens of *Spiniferites cruciformis* and *Seriliodinium explicatum* with cruciform endocysts; however, the meaning of the term 'rounded cruciform' was not further defined. Jimenez-Moreno et al. (2006) used the adjective rhombo-cruciform to describe the rounded cruciform proximate cyst of a *Pyxidinopsis* sp. from the Langhian Stage of the Pannonian Basin (here including Vienna Basin), in the western Paratethyan Sea region (see Figure 2). It appears that the terms rounded cruciform, sub-cruciform and rhombo-cruciform refer to endocysts or autocysts with less strongly concave sides above and below the cingular area and lacking strong dorsoventral compression.

2.1.2. Pterate

Pterocysta cruciformis superficially resembles *Spiniferites cruciformis* in having a strongly cruciform endocyst but it has a very different outer wall development, with only the middle section of the ventral surface (the sulcal area) being covered by a perforate, wing-like structure formed by separation of the endophragm and ectophragm (Figures 1.3, 1.6). The generic name *Pterocysta* is derived from Greek *pteryx* (wing) and *-cysta*. Earlier, Balteş (1971) described *Thalassiphora balcanica* (a.k.a. *Spiniferites balcanicus*) as a pterate cyst bearing a membranous 'lamellate wing' formed by the periphragm but he did not define the term. Williams et al. (2002) also use the adjective 'pterate' for cysts with processes linked distally or in a mesh-like fashion to form a wing or flange in the equatorial zone. Here we broaden the use of 'pterate' to include the vertically-aligned, wing-like ectophragmal structure found in the camocavate cyst *Pterocysta cruciformis*. This structure is sometimes referred to as a crest (Rochon et al. 2003) but we now avoid use of the term 'crest' because in a strict sense, it refers to parasutural structures, including lists and wide septa (see Fensome et al. 1993 and Williams et al. 2002), as found in the proximo-chorate/chorate cyst *Spiniferites cruciformis*.

2.1.3. Galeate

Galeacysta derives its name from the Latin word *galea* = helmet and *-cysta,* with reference to the perforate and claustrate (trellis-arched) periphragm covering the sides of the ventral endocyst surface (Corradini and Biffi 1988). Galea (plural galeae) refers to a Roman or Mediaeval soldier's helmet which has various large arch-shaped openings and often has a crested top in contrast to a smooth, bowl-shaped motorcycle crash-helmet. Williams et al. (2000) use the adjective 'galeate' for acritarchs characterised by a 'hemispherical outline and a polar excystment aperture' as proposed by Servais and Eiserhardt (1995, p. 192); this inflated bowl shape does not include large arched openings as in a soldier's helmet. We apply the term galea and its adjective galeate as first introduced by Corradini and Biffi (1988) to indicate gonyaulacoidean dinoflagellate cysts with a helmet-shaped claustrate periphragm that over-arches the sides of the ventral endocyst surface.

2.2. Spiniferites cruciformis *Wall and Dale 1973*

2.2.1. Spiniferites cruciformis *holotype and paratypes.*

The holotype of *Spiniferites cruciformis* is from Late New Euxinic (Neoeuxinian) Stage sediments of R/V Atlantis II 1969 Core 1451G on the upper slope of the northwestern Black Sea (Wall et al. 1973). The Late New Euxinic Stage interval

approximately corresponds to the latest Pleistocene – earliest Holocene (ca. 17,000 to 9,000 yr BP). Originally, this palaeoenvironment was qualitatively described as being fresh due to the influx of glacial melt water. However, quantitative studies from other sites on the southwestern Black Sea shelf show that the surface water salinity (SSS) was 7 – 13 psu (practical salinity units) during this time (Mertens et al. 2012; Bradley et al. 2013). This salinity, which corresponds with peak relative abundances of *Spiniferites cruciformis*, is in the brackish water range (see Figure 2).

Spiniferites cruciformis is a typical proximochorate/chorate cyst with gonyaulacacean tabulation characteristic of *Spiniferites* and normally with well-developed gonal processes in the lateral equatorial and the polar areas. The archeopyle is precingular P(3″) with a free operculum. The holotype of *Spiniferites cruciformis* (Wall et al. 1973, pl. 1, figs. 2–3) is illustrated by light micrographs (LM) showing dorsal and ventral surfaces of the endocyst in equatorial view and clearly demonstrating the notably concave epicyst and hypocyst ambital profiles, and the dorsoventral compression of a typical cruciform cyst. The holotype images display a specimen with well-developed ornament on the hypocyst, particularly in the left ventral area where the sutural membrane is almost as wide as the endocyst diameter; elsewhere, however, the sutural membranes are reduced. This uneven development of the septa gives the specimen an asymmetrical outline (referred to as *Spiniferites cruciformis* form 2 by Mudie et al. 2001; see Plate 1 and Table 1). The holotype also shows characteristically large cingular lateral processes with flared bi- to trifurcate tips and connecting membranous sutural septa that form rectangular box- or trumpet-shaped structures in specimens with normally developed (i.e. long) processes (e.g. Plate 1, Figures 5 and 9). Other typical features of the cruciform endocyst are the rounded polar apices, with the epicyst being narrower than the hypocyst, and with a small apical boss but flat antapical area. The ornament is characteristically best developed in polar, lateral cingular, lateral and intercalary posterolateral areas. The sulcus is broader than in most *Spiniferites* species and the posteroventral endocyst surface includes an almost square posterior sulcal platelet area (ppl) at the mid-ventral base adjacent to the posterior intercalary area (Ip) that is often surrounded by well-developed flanges. Two conspicuous sutural septa also connect the ppl and Ip.

Specimens from a deeper water core (Atlantis II, 1445P) were used to illustrate other features of this first-described cruciform dinoflagellate cyst (Wall et al. 1973). LM images of a specimen in apical view (ibid pl. 1, fig. 5) show the characteristic dorso-ventral compression of a cruciform cyst, and the pentagonal dorsal plates 2′ and 3′ which are clearly outlined by wide septa although the two small ventral plates are less visible. Another LM image (ibid pl. 1, fig. 6) shows a variant with strongly reduced ornament as seen in equatorial view. Notable features of this morphotype are well-defined sutural traces in lateral areas and around the almost quadrangular antapical plate; these features correspond to those of *Spiniferites cruciformis* form 4 of Mudie et al. (2001). Scanning electron microscope images (SEMs) of the Wall et al. (1973) paratypes in dorsal view (ibid pl. 2, figs. 1 and 2) show essentially the same features as the holotype but additionally reveal variable amounts of septal perforation and scabrate to finely corrugate endocyst wall surface with a 'beaded' texture. The SEM image in ventral view (Wall et al. 1973, pl. 2, fig. 3) shows a specimen with reduced ornament but still retaining the characteristic transverse posteroventral septum that Eaton (1996) considered a key characteristic distinguishing *Spiniferites cruciformis* from *Seriliodinium explicatum*. The other SEM image (ibid pl. 2, fig. 4) provides an oblique dorsal view of a specimen with strongly suppressed septa development, described as having spinose ornamentation. This morphotype largely corresponds to *Spiniferites cruciformis* form 3 of Mudie et al. (2001) but it differs in showing traces of a single trabeculum linking the left lateral epicystal processes.

2.2.2. Spiniferites cruciformis *in the Ponto-Caspian Seas and freshwater lakes.*

Spiniferites cruciformis displays the widest range of variation in ornament of the three key taxa assigned to the '*Galeacysta etrusca* complex', but it is usually easily distinguished by its cruciform or subcruciform to pyriform (pear-shaped) endocyst outline, vestigial (small remnant) processes, wide ventral membranous flanges, and absence of galeate or pterate periphragm ornament. Forms with reduced ornament are always distinguishable by the presence of parasutural traces and vestigial septa on the ventral surface. Figure 4 and Table 1 summarise the typical characteristics and salinity ranges of the morphotypes in modern semi-marine to brackish environments and the features of the cysts in freshwater lakes as described in more detail as follows.

Since 1973, there have been many reports of the occurrence of *Spiniferites cruciformis* in sediments from late Miocene to modern age within the geographic region from Spain and the Alboran Sea in the western Mediterranean (Popescu et al. 2007, Do Couto et al. 2014, Popescu et al. 2015) to the Aral Sea, Central Asia (Marret et al. 2004, Sorrel et al. 2006, Leroy 2010). Most of these studies, however, do not provide illustrations or descriptions of the species which would allow us to determine the full range of morphological variation, and some images show Miocene specimens that seem to be incorrectly identified (see Sect. 2.3.1). Here we focus on studies that provide details of specimens for the Ponto-Caspian Seas (including Marmara, Black, Azov, Caspian and Aral Seas) and a few freshwater lakes (Figure 2). We start with the seas which presently have some Aegean normal marine seawater influence: the semi-marine Marmara and low salinity marine Black Seas. We then progress eastwards to the endorheic Caspian and Aral Seas that have received only river drainage since Pliocene time, and finally, to studies of *Spiniferites cruciformis* in freshwater lakes.

In the semi-marine Marmara Sea (mean annual SSS 20-25, Na 8.1 mg/l, $MgSO_4$ ~8 mg/l) and the low salinity marine Black Sea (mean annual SSS 16-18, Na 5.4 mg/l, $MgSO_4$ 7.1 mg/l), *Spiniferites cruciformis* is abundant (about 20 – 80% of cysts counted/sample) in sediment of Late Pleistocene (MIS 3 and 2) to mid-Holocene age (ca. 6.5 cal ka, about 2,500 years

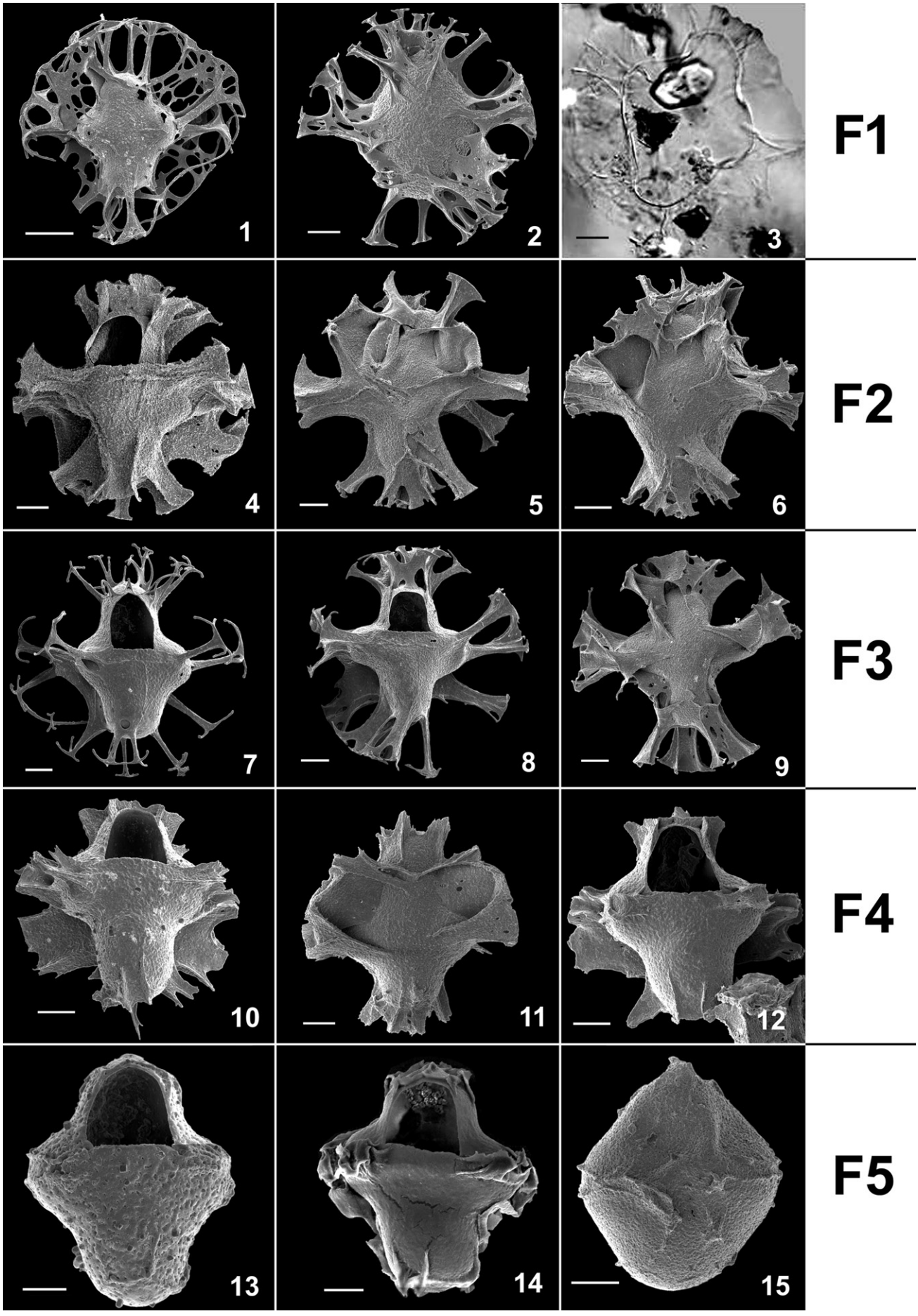
1
2
3
F1
4
5
6
F2
7
8
9
F3
10
11
12
F4
13
14
15
F5

after the New Euxinian Stage), and then it becomes sporadically present in low amounts (mostly <3%), as also seen in its modern distribution within the Ponto-Caspian region (Mudie et al. 2001, 2002, 2004; Mudie et al. 2017). The range of cyst morphology observed in 180 specimens from Late Glacial sediment at the paratype site in the southeastern Black Sea (Plate 1) and in Marmara Sea (Plate 2, Figures 1–3) is essentially the same as that reported by Wall et al. (1973) for the western Black Sea sediments of the same age. The specimens in Plate 1 show the range of variation in endocyst surface texture found within a single sample from Atlantis II core 1474P at the Black Sea paratype site: most endocyst surfaces are scabrate but rare psilate and corrugate specimens are also present.

The five Marmara Sea *Spiniferites cruciformis* morphotypes called *Spiniferites cruciformis* forms 1 – 5 by Mudie et al. (2001) are clearly recognised in the southeastern Black Sea paratype assemblages (Plate 1, Table 1). *Spiniferites cruciformis* form 1 has long (ca. 50% of the endocyst diameter), well developed processes on both epicyst and hypocyst, giving it a spherical outline (Plate 1, Figures 1–3); *Spiniferites cruciformis* form 2 also has well-developed ornament but the septa are unevenly developed, giving it a strongly asymmetrical outline (Plate 1, Figures 4–6); *Spiniferites cruciformis* form 3 has long processes but suppressed septa development, giving it a spinous outline (Plate 1, Figures 7–9); *Spiniferites cruciformis* form 4 has reduced processes <25% of the endocyst diameter (Plate 1, Figures 10–12); *Spiniferites cruciformis* form 5 has strongly reduced processes, sometimes evident only as cingular and other discontinuous low septal ridges in dorsal view, and in ventral view, as lateral cingular septal ridges and usually, traces of the sulcal ornament (Plate 1, Figures 13–15).

Statistical analysis of endocyst length:width shape measurements of the five *Spiniferites cruciformis* forms does not reveal any correlation with morphotype group (Figure 3A). Relative abundances of the combined forms and SSS as determined from planktonic foraminiferal $\partial^{18/16}O$ values in the same samples from Marmara Sea Core MAR94-5 show very weak correlation (Mudie et al. 2001) but there is correlation of $R^2 = 0.67$ (at p 0.1) for *Spiniferites cruciformis* form 1 within a SSS range of 11 – 19 psu (Figure 3B). This salinity range is close to its modern mean annual salinity range throughout the marine-lacustrine basins of the Ponto-Caspian region (Mudie et al. 2017). Rare specimens in modern surface samples of the semi-marine Marmara Sea (Plate 2, Figures 1–2) and the northern low salinity marine Black Sea (Plate 2, Figures 5–6) are morphotypes with well-developed ornament (forms 1 and 2).

In the brackish waters of the endorheic Central Asian Caspian (SSS 1.2 – 13, Na 3.2 mg/l, $MgSO_4$ 23.6 mg/l) and northern Aral Seas (SSS 9 – 11, Na 2.2 mg/l, $MgSO_4$ 23.3 mg/l prior to the severe desiccation beginning in 1960), *Spiniferites cruciformis* is a significant component of the microplankton association throughout the late Neogene and Quaternary. The oldest confirmed records are from late Miocene (Pontian) exposures in the Kirmaky Valley, Azerbaijan (van Baak 2015). Overlying sediments of the Kirmaky Suite are dated as early Pliocene (Zanclean) based on magnetostratigraphy (van Baak 2015) and these fluvio-lacustrine beds contain occasional *Spiniferites cruciformis*, in association with *Caspidinium rugosum* Marret in Marret et al. 2004 and varied numbers of freshwater algae (Richards 2012). *Spiniferites cruciformis* is then rare but consistently present within the sediments of the Pliocene Productive Series (Richards et al. 2014a) and becomes locally abundant during the Pleistocene (Richards et al. 2011, 2014a, b and new data shown in Sect. 3).

The most detailed morphological studies of *Spiniferites cruciformis* from the Caspian Sea are for cysts in the warmer, more saline waters of the central and southern basins (Marret et al. 2004), with other information on abundance and distribution given by Leroy (2010), and Leroy et al. (2007, 2013, 2014). In this region, associated summer SSS ranges from 1.5 – 5 in Lake Anzali to 13 in most areas, with a maximum value of 15 psu; here *Spiniferites cruciformis* is widespread in low to moderately high numbers in surface samples. As in the Black Sea, this cruciform species is locally abundant in late Pleistocene – early Holocene sediments (Leroy et al. 2014); however, it is also present (ca. 2–20%) in modern sediments of the central and southern Caspian Sea basins and adjoining bays. The bays include the Kara-Bogaz Gol (SSS 13 – 28, Na 5.35 mg/l) which is the world's largest $NaSO_4$ water body (Zenkevitch 1963) and has up to 6% *Spiniferites cruciformis*; however, the highest amounts (40%) occur in the lower salinity (1.5 – 1.75 psu) Lake Anzali (Kazancı et al. 2004, Marret et al. 2004). *Spiniferites cruciformis* also occurs (up to 17%) in the brackish water and saltflats of late Holocene and surface sediment of the Aral Sea (Sorrel et al. 2006, Mudie et al. 2017).

In both the Caspian and Aral Seas, *Spiniferites cruciformis* occurs in low diversity cyst assemblages dominated by *Lingulodinium machaerophorum* (Deflandre and Cookson 1955) Wall 1967 and *Impagidinium caspienense* Marret in

Plate 1. SEM images and a LM image (Figure 3) of *Spiniferites cruciformis* from Late Pleistocene sediment, 14.5 m core-depth (250 – 252 cm core depth in section C33-32A) at the paratype site Atlantis II Site 1474P in southeastern Black Sea, showing the wide range of morphology in one population, grouped into the forms of Mudie et al. (2001). Scale bar = 10 μm. Figures 1–3: *Spiniferites cruciformis* form 1 with an essentially rounded periphragm outline. 1. ventral view of specimen with maximally developed ornament, including some single trabeculae and with reduced transverse posterior epicyst septa, as found in *Seriliodinium explicatum*. 2. Ventral view of a rare specimen a sub-cruciform endocyst outline. 3. LM of typical specimen in optical section. Figures 4–6: *Spiniferites cruciformis* form 2. 4. Dorsal view of specimen with hypotractal septal flanges; 5. Ventral view of specimen with two epicystal flanges; 6. Ventral view of specimen with only one septal flange (right epitractal position). Figures 7–9: *Spiniferites cruciformis* form 3. 7. Dorsal view of specimen with all septa suppressed except in the right epicystal area. 8. Dorsal view of specimen with suppressed septa except in apical and right epicystal areas. 9. Ventral view of specimen showing reduced septa around the 1p and ps plate areas. Figures 10–12: *Spiniferites cruciformis* form 4. 10. Dorsal view of specimen with hypotractal flanges; 11. Ventral view of specimen with epitractal flanges; 12. Dorsal view of specimen with more reduced ornament than in Fig.10. Figures 13–15: *Spiniferites cruciformis* form 5. 13. Dorsal view of specimen with extreme reduction of septa and with corrugate wall surface. 14. Dorsal view of rare almost psilate specimen with low membranous septa on the hypotract. 15. Ventral view of rare morphotype with rhomboidal body; note the parasutural traces in paracingular and parasutural areas that distinguish this morphotypes from reduced forms of *Galeacysta*. All SEM images by AR; LM image 3 of PJM.

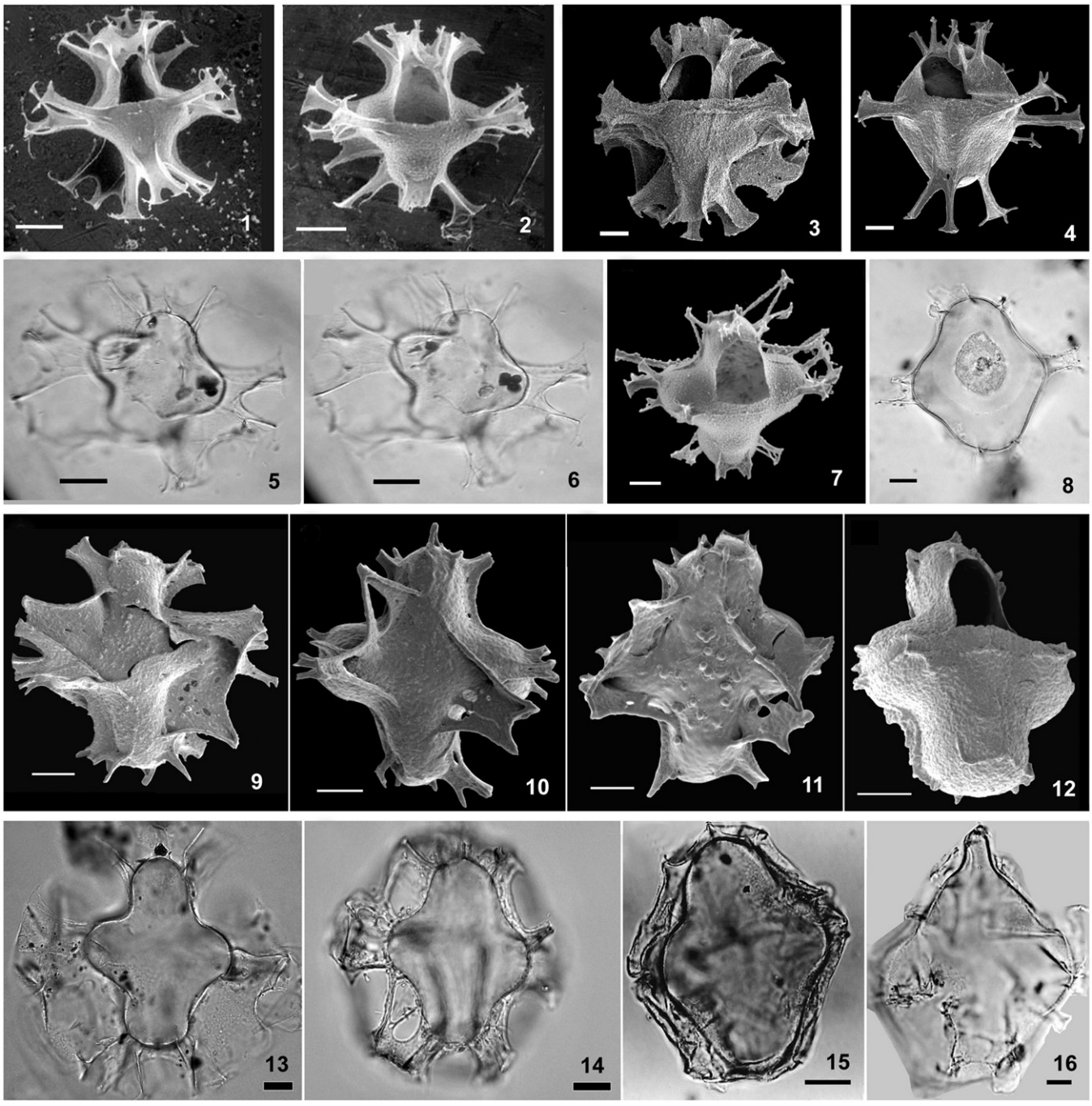

Plate 2. SEM and LM images of *Spiniferites cruciformis* from Marmara Sea (Figures 1 – 4), the Black Sea (Figures 5 – 6 surface sediment; Figure 7 MIS 3), a freshwater lake (Figure 8), northeastern Caspian Sea, Emba Delta (Figures 9 – 12) and offshore Caspian Sea basins (Figures 13 – 16). Scale bar = 10 μm. Figures 1 – 2: SEM images of *Spiniferites cruciformis* form 3 from Marmara Sea core MAR 94-5, 140 cm depth, in dorsal view and showing the variation in endocyst surface texture from scabrate (1) to finely corrugate (2) and in the amount of septa reduction between processes. Figures 3 – 4: SEM images of *Spiniferites cruciformis* from late Pleistocene in Core MAR89P, 260 cm, Marmara Sea. 3. Dorsal view of *Spiniferites cruciformis* form 2 showing details of box-like complex processes in the lateral girdle region. 4. Dorsal view of sub-rhomboidal specimen similar to those reported for Turkish lake sediments. Figures 5 – 6: LMs of *Spiniferites cruciformis* form 1 from surface sediment (sample H 42, 0-2 cm) in the northwestern Black Sea. 5. Ventral view in high focus. 6. optical section. Figure 7: SEM of *Spiniferites cruciformis* form 3 specimen from late Pleistocene sediment, SW Black Sea: dorso-apical view, showing pericoel openings and variability of process structure. Figure 8: LM of specimen of *Spiniferites cruciformis* form 3 from near-surface sediment (9 cm depth) in Lake Sapanca (from SAG Leroy, SA03k71_9_spincrucif_1); optical section. Figures 9 – 12: SEM images from late Pleistocene sediment off the Emba Delta, Caspian Sea. 9. Ventral surface of form 2 specimen, with scabrate to microverrucate endocyst surface. 10. Ventral surface of different form 2 specimen with reduced ornament and pitted endocyst wall texture. 11. Ventral surface of *Spiniferites cruciformis* form 2 specimen with a coarsely verrucate endocyst wall surface. 12. Dorsal surface of morphotype c with a cruciform endocyst and strongly reduced processes and parasutural septa. Figures 13 – 16: LM images of Caspian Sea morphotypes in optical section view (from SAG Leroy). 13. *Spiniferites cruciformis* Morphotype A with typical cruciform endocyst and well-developed ornament; US0-2-2, 0 cm, ventral view, mid-focus. 14. *Spiniferites cruciformis* Morphotype B with slightly reduced cruciform shape and reduced septa, Core CP04, 0-2.5 cm. 15. *Spiniferites cruciformis* Morphotype C, showing reduced cruciform endocyst shape and suppressed process formation; Core GS05, 5 – 6 cm. 16. *Spiniferites cruciformis* Morphotype C with pyriform endocyst and vestigial ornament; Core GS05, 5 – 6 cm. SEM Images of AR except as shown; LM images of PJM except for images 8 and 13 – 16 kindly contributed by Suzanne Leroy.

Table 1. Characteristic features of *Spiniferites cruciformis* morphotypes and their distribution in modern surface sediments as indicated by colour coding of the following locations: M Marmara Sea; B Black Sea; C Caspian Sea; A Aral Sea; L freshwater lakes

Spiniferites cruciformis Morphotype	Cyst type	Ambitus of peripragm	Ambitus of endocyst	Processes	M	B	C	A	L
Form 1		Spherical	Cruciform						
Morphotype A	Chorate Up to 50% endocyst	Spherical to subspherical	Cruciform to pyriform	Prominent gonals box-like, linked by wide septa, rarely trabeculate					
Form 2		Subspherical	Cruciform						
Form 3 and Morphotype B	Proximochorate 10-30% endocyst	Spinate and irregular	Cruciform	Spinate gonals, Low/no septa					
Morphotype C	Pseudo-proximate to proximate	NA	Cruciform to pyriform	Low crumpled or folded processes					
Form 4	Sub-proximate 5-10%	NA	cruciform to rhomboidal	Low septa and short processes					
Form 5	Proximate	NA	cruciform to sub-cruciform	Sutural and sulcal ridges only					

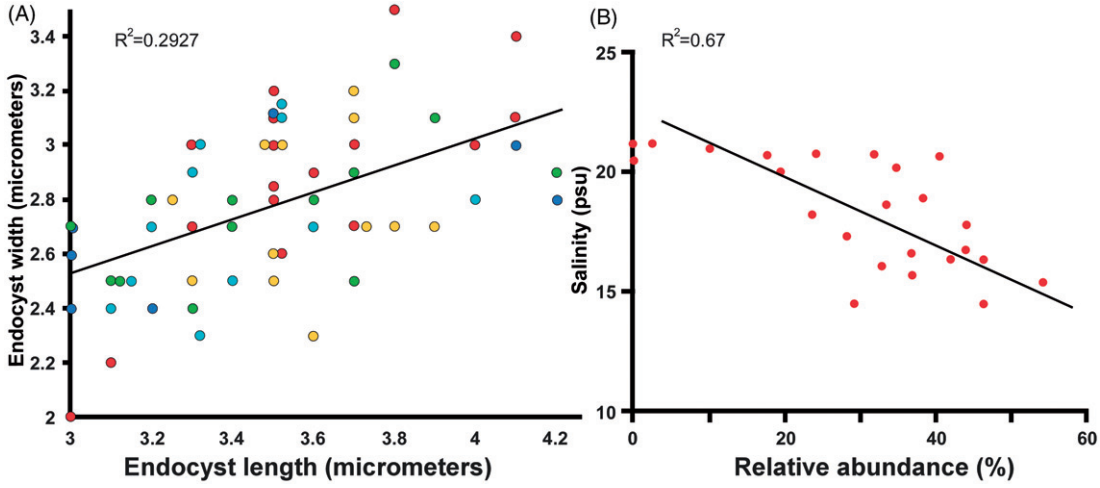

Figure 3. *Spiniferites cruciformis* morphotypes from early Holocene sediment in Marmara and Black Sea: A. Relationship between endocyst length and width among the five forms in late-Pleistocene – early Holocene interval of Marmara and Black Sea. B. Correlation between sea surface salinity (SSS) of planktic foraminifera (measured from $\delta^{18/16}O$ isotope ratios) and the relative abundances of *Spiniferites cruciformis* form 1 in Marmara Sea core MAR 94-5.

Marret et al. 2004, commonly with lower amounts of cysts of *Pentapharsodinium dalei* Indelicato & Loeblich III 1986 and *Caspidinium rugosum*. Marret et al. (2004) described three morphotypes in samples from central to southern Caspian Sea (summarised here in Table 1). *Spiniferites cruciformis* Morphotype A has a cruciform endocyst and a conspicuous membranous flange in ventral view (see Marret et al. 2004, pl. IV, figs. 1–5; pl. V, fig. 4); it displays the same features and range of septa development and perforation as shown for the Black Sea forms 1 and 2 (Plate 2, Figures 13–14), but sometimes there is a conspicuous apical boss in place of the typical rounded surface and the sutural membranes are widely perforate to fenestrate. This is the most widespread morphotype and it comprises 10 – 20% of total cysts in the southern deep basin of the Caspian Sea (Leroy et al. 2007) and in most samples from the northern Aral Sea (Sorrel et al. 2006, fig. 7, images 7.5 – 7.12). It is also subdominant with *Lingulodinium machaerophorum* and *Impagidinium caspienense* in the brackish water phase of the Langarud wetlands ca.1 ka BP, located near Anzali lagoon, but it disappears along with minor occurrences of Morphotypes B and C in the freshwater phase (Haghani et al. 2015). It is sparingly present in the low salinity (0.2 – 11 psu) waters of the Volga and Emba river areas of the northernmost Caspian Sea (Plate 2, Figures 9–11) where sea ice forms in winter.

Spiniferites cruciformis Morphotype B has a cruciform endocyst with reduced septal membranes and essentially corresponds to the Black Sea form 3 (Marret et al. 2004, pl. IV, figs. 6–9; pl. V, fig. 5) except it is sometimes subcruciform, with an apical boss. This subcruciform morphotype is confined to the deep southern basin of the Caspian Sea where it may comprise up to 20% of the assemblage. Morphotype C of Marret et al. (2004) is characterised by a less pronounced cruciform endocyst shape than the holotype and has processes which are usually short, straight, lack terminations and are folded on the endocyst (Plate 2, Figure 15). There are no wide membranous flanges between the processes but in dorsal view, the sides may appear covered by low septal

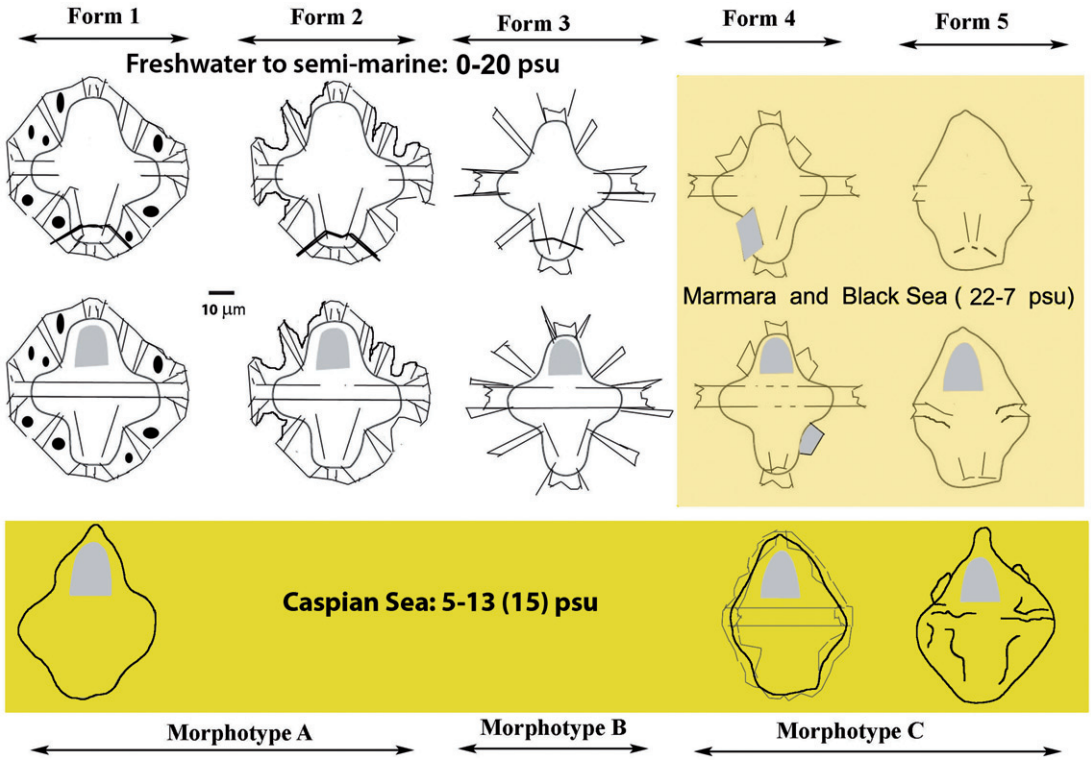

Figure 4. Sketches showing the key features of *Spiniferites cruciformis* morphotypes (adapted from Marret et al. 2004) in ventral and dorsal views and their relation to surface water salinity in Holocene to recent sediments of the Ponto-Caspian Seas. The pyriform Caspian Sea morphotype in column 1 is shown without ornament which is the same as the cruciform morphotypes illustrated above it. Gray shaded areas denote archeopyles and septal flanges in forms with reduced ornament; black ovals denote perforations. Bottom yellow rectangle is color-coded to Figure 2; the orange rectangle includes late Pleistocene – early Holocene morphotypes and their derived salinity range; the other morphotypes (unshaded area) occur in semi-marine to freshwater locations.

membranes, similar to *Spiniferites cruciformis* form 4 (Plate 2, Figure 15). The apical boss of Morphotype C commonly is very prominent, giving the endocyst a pyriform shape (Plate 2, Figure 16) which is also seen in *Spiniferites bentorii* subsp. *oblongus* Sütő-Szentai 1986. These pyriform morphotypes are also confined to deep water of the southern basin where it is less common (maximum 10%) than the other Caspian morphotypes. The most highly reduced *Spiniferites cruciformis* form 5 has not been recognised in the Caspian Sea and conversely, the pyriform Morphotype C has not been reported for the Black Sea.

Modern freshwater lakes apparently contain only *Spiniferites cruciformis* morphotypes with cruciform endocysts and reduced sutural septate ornament (Plate 2, Figure 8), as found in surface sediment of Lake Sapanca southeast of Marmara Sea (Leroy and Albay 2010) and in Lake Terkos near Istanbul (KN Mertens, pers. communication 2010). In Lake Sapanca, *Spiniferites cruciformis* is associated with *Brigantedinium* and *Impagidinium caspienense*. For the late Pleistocene – early Holocene interval of Lake Kastoria in northwestern Greece, however, *Spiniferites cruciformis* co-occurs exclusively with the freshwater species *Gonyaulax apiculata* Entz 1904 (Kouli et al. 2001). These assemblages display a wide range of endocyst shapes from cruciform to ellipsoidal-pentameral, **w**ith rare occurrences of intermediate forms. Sutural ornamentation of these populations is similar to that of *Spiniferites cruciformis* forms 1 to 3 but conspicuously does not include the forms 4 and 5 with strongly reduced ornamentation. Kouli et al. (2001) also found that endocyst size appeared to be independent from sutural membrane development and there tended to be a predominance of either cruciform or ellipsoid cysts in the lake sediments. For one Pliocene interval in another freshwater Greek lake, Lake Ptolemnais, Kloosterboere-van Hoeve et al. (2001, pl. 1 a – d) illustrate a taxon they called *Spiniferites cruciformis* but which has only ellipsoidal to rhomboidal endocysts. These freshwater cysts are also exclusively co-associated with *Gonyaulax apiculata* but they differ conspicuously from the Lake Kastoria and the extant *Spiniferites cruciformis* morphotypes in bearing only short processes which tend to be concentrated along the paracingular area. It appears that these ellipsoid Pliocene Lake Ptolemnais cysts are a different species than *Spiniferites cruciformis*.

2.3. Galeacysta etrusca *Corradini and Biffi 1988.*

2.3.1. Galeacysta etrusca *holotype and topotypes*

The holotype of *Galeacysta etrusca* is from a thin, organic-rich mud layer at the top of a sandy bed (Unit C) in the Late Messinian Cava Serredi section of Tuscany in northwestern Italy (Corradini and Biffi 1988). Based on foraminifera, molluscs, ostracods and charaphytes, the palaeoenvironment was interpreted as a shallow lacustrine basin of variable salinity and characteristic of the Mediterranean Lago-Mare biofacies. *Galeacysta etrusca* was the dominant species in a low diversity dinocyst assemblage, co-occurring with two *Impagidinium* species designated as *Impagidinium* sp. 1 and *Impagidinium* sp. 2. According to Popescu et al. (2007), the Lago Mare biofacies no longer has a regional chronostratigraphic sense, and '… .should be understood as the invasion of Paratethyan

organisms via surface waters owing to a connection at high sea-level between the Aegean Sea'. In that paper on the latest Messinian Maccarone section of northwestern Italy, Popescu et al. (2007, p. 364) report that they made particular effort to identify the brackish stenohaline Paratethyan species *Galeacysta etrusca*, *Romanodinium areolatum* Balteş 1971, *Spiniferites balcanicus* Sütő-Szentai 2000 (= *Thalassiphora balcanica)*, *Spiniferites bentorii* subsp. *pannonicus* Sütő-Szentai 1986, *Spiniferites cruciformis*, and *Spiniferites galeaformis* Sütő 1994 (amongst 20 other Paratethyan taxa) by directly comparing the Maccarone specimens with topotypes of these and by examining their original iconography and description. As a result, Popescu et al. (2007) concluded that the *Impagidinium* sp. 2 of Corradini and Biffi (1988, pl. 3, figs. 1–6), also illustrated by Bertini (1992: pl. 3, fig. 9), is a morphotype of *Spiniferites cruciformis* by reference to illustrations by Marret et al. (2004) and Mudie et al. (2004). In fact, the specimens in the LM images of Corradini and Biffi (1988) have neither cruciform endocysts nor do they have the characteristic sutural ornament of *Spiniferites cruciformis* forms 1 – 4 (see Sect. 2.2). One of the two *Impagidinium* sp. 2 specimens of Bertini (1992) has box-like membranous processes in lateral view but the endocyst is not clearly cruciform. In the absence of further documentation, it remains uncertain that the holotype of *Galeacysta etrusca* co-occurs with *Spiniferites cruciformis* at the type locality. This is an example of how errors in the identification of the marker taxa may enter the scientific literature and begin to blur the records of cruciform cyst occurrences in time and space.

The genus *Galeacysta* as defined by Corradini and Biffi (1988) is a camocavate cyst with an ellipsoidal endocyst and ellipsoidal to subpolygonal 'pericyst' (called an ectocyst in the current manuscript) that gives it a distinctly different outline compared to almost all morphotypes of *Spiniferites cruciformis*. The endophragm and periphragm are adpressed dorsally but are widely separated in the ventral region, forming the galeate periphragm which is entirely absent over the sulcal area. The holotype endocyst surface is smooth throughout but the periphragm is smooth to finely granulate and is irregularly perforate or fenestrate. Gonyaulacoid paratabulation is indicated by raised sutural ridges on the dorsal surface and by intratabular periphragm claustra (here meaning large arched openings as in trelliswork, not a general name for openings/tears as cited by Evitt, 1985). As in *Spiniferites cruciformis*, the archeopyle is precingular P(3″) with a free operculum.

The holotype of *Galeacysta etrusca* Corradini and Biffi 1988 is illustrated by LMs (Plate 3, Figures 1–4) which show lateral and ventral views of a relatively large cyst (endocyst 52 x 66 μm; ectocyst 78 x 80 μm). The type specimen has an ellipsoidal endocyst without significant dorsoventral compression (width:thickness = 0.79) and with wide separation of the ectophragm in the ventro-lateral region to form the characteristic fenestrate galea that enfolds the apical area and sides of the atabular, smooth-walled ventral surface (Corradini and Biffi 1988, pl. 1, figs. 1–4, 9; pl. 2, fig. 2) but does not cover the sulcal area (except in squashed specimens e.g. ibid pl. 1, figure 11). The average length to width ratio of this ellipsoid endocyst is <1.2 (82 specimens). The periphragm surface is smooth to finely granulate. The lateral and dorso-apical surfaces of the cyst in SEM images (ibid. pl. 2, figs. 1 and 4) display a variably perforated, fenestrate periphragm attached on the sides of the dorsal and polar areas from which it extends ventro-laterally as reproduced here in Figure 1.1 and Plate 3, Figures 1–3. According to Corradini and Biffi (1988), the perforations correspond to paratabulation so that the large periphragm 'trellises' (claustra) outline paraplates. In dorsal view, paratabulation is clearly indicated by sutural ridges in the precingular, cingular and postcingular plates areas, with the paracingulum being well-defined by narrow membranous septa. The apical plates have insert organisation, so that there is no contact between plates 2′ and 4′. The antapical plate is reported as appearing quinqueform (ibid pl. 1, fig. 12), and Corradini and Biffi (1988) state that the ps and p plates are evident in their LM images (pl. 1, fig. 6 and pl. 2, fig. 7); however, illustrations of these features are not clear. The authors emphasise that the sulcal area 'is characterised by absence of the periphragm and unrecognisable paratabulation'.

Overall, the notable features distinguishing the holotype of *Galeacysta etrusca* from *Spiniferites cruciformis* and its morphotypes are the consistently ellipsoidal endocyst bearing the galeate periphragm which is attached dorsolaterally and apically by membranes and hollow processes, lack of tabulation on the ventral surface, the relatively low (<25% body width) membranous sutural septa seen in dorsal and ventral equatorial views, and the well-defined continuous cingulum outlined by raised sutural ridges or low septa on the dorsal surface. Corradini and Biffi (1988) comment that *Galeacysta etrusca* differs from *Lophocysta* Manum 1979 by 1) the presence of parasutural ridges on dorsal and ventral endocyst surfaces except the sulcal area; 2) the absence of gonal 'processes' in the dorsal area; 3) the presence of trellis-like perforations on the periphragm. They also comment that there is some similarity to *Thalassiphora* Eisenack & Gocht 1960, emend Gocht 1968, especially *Thalassiphora delicata* Williams & Downie 1966 but *Thalassiphora* differs in not having weakly defined paratabulation and trellis-like periphragmal plate outlines, and in having the sulcal area entirely covered by the bowl-shaped periphragm. It can also be noted that the plate formula for *Thalassiphora pelagica* (Eisenack 1954) Eisenack & Gocht 1960, emend. Benedek and Gocht 1981 (4′, 6″, 0c, 5‴, 1⁗, s) differs from that of *Galeacysta etrusca* (4′, 6″, 6c, 6‴, 1p, 1 ps, 1⁗), and the periphragm of *Galeacysta etrusca* is not formed by stretching of a ventral spongy or foamy outer wall comprising folded and twisted membranes covered by a thin tectum, as described by Benedek and Gocht (1981) for *Thalassiphora pelagica*. In *Galeacysta etrusca,* the endocyst and ectophragm walls appear to be thin although both can be covered by finely tegillate surface ornament (Plate 3, Figures 13, 18). This tegillum is not developed by stretching of wall luxuria elements as in the skolochorate cyst wall model of de Verteuil and Norris (1996).

2.3.2. *Galeacysta etrusca* in the Mediterranean, Pannonian Basin and Ponto-Caspian Seas.

Subsequent to the work of Corradini and Biffi (1988), cysts identified as *Galeacysta etrusca* were variously reported as

being widespread in brackish waters of the Paratethyan Seas and possibly intergrading in a complex of five genera, including *Spiniferites balcanicus* (=*Thalassiphora balcanica* in this paper), *Spiniferites cruciformis, Romanodinium areolatum* and *Nematosphaeropsis bicorporis* Sütő-Szentai 1990 (Popescu et al. 2009 and references therein). In a morphological study of *Galeacysta etrusca, Spiniferites balcanicus* and *Romanodinium areolatum* from various well-dated Mediterranean and Paratethyan sections, Popescu et al. (2007) also concluded that these taxa probably represented different steps in evolution/adaptation to environmental changes (probably in surface water salinity) of a single species and they were grouped together with *Galeacysta etrusca* in one graphical curve as an index of low salinity. These authors also note that specimens they identified in the Maccarone section as *Spiniferites cruciformis* and *Pyxidinopsis psilata* (Wall & Dale in Wall et al. 1973) Head 1994 show a wide range of morphologies as reported for Black Sea Holocene populations by Wall et al. (1973). Within the Messinian event, Bertini et al. (1995), Bertini (2006 and personal communication, 2016) also found a very wide range in size and ornamentation of *Galeacysta etrusca* from typical morphotypes to 'a *Spiniferites cruciformis* type'. Popescu et al. (2007) consider that cyst data for the entire Neogene and Paratethys interval reveal a transition from oval to cruciform body, and that '… the well- to poorly-expressed tabulation characterizes reduced surface-water salinity'. Unfortunately, there are no illustrations to demonstrate the meaning of 'well- to poorly expressed tabulation' but 11 of 12 images in a subsequent paper (Popescu et al. 2009) display prominent ridges and narrow septa continuously present along the dorsal cingulum which is typical of *Galeacysta etrusca* but is absent in the cruciform species *Spiniferites cruciformis* (Plates 1 and 2) and *Pterocysta* (Plate 4).

Four ecotypes are recognised and illustrated in a biometrical study of >1100 specimens of the '*Galeacysta etrusca* complex' by Popescu et al. (2009, pl. 2, figs. 1–12) but few of the images show the lateral or ventral views needed to correctly identify *Galeacysta etrusca,* including the specimen used to demonstrate the key parameters employed for statistical analysis of endocyst:ectocyst (EN:EC) ratios (ibid, pl. 1). In Plate 3 (Figures 7, 11–12, 15 – 17), we reproduce the specimens that are shown in ventral or lateral view, thereby allowing certain identification. Popescu et al. (2009) used log-transformed ratios of EN:EC to delimit four ecological groups within the *Galeacysta etrusca* complex. The statistically defined group 'a' includes specimens from the Dacic and Krašić Paratethyan basins (Plate 3, Figure 11) and the Lago-Mare bed in the Maccarone Section (Plate 3, Figure 17) and is considered to characterise brackish environments. The SEMs of these taxa reveal the presence of an attached operculum on both specimens, and more reduced periphragm separation in the Pannonian specimens than in the type and topotype specimen from Mediterranean basins as shown in Figure 1 and Plate 3, Figures 1–4. The ecological group 'c', represented by cysts from the Majs 2 site in the Pannonian basin (Plate 3, Figures 12, 15) is interpreted as a similar environment but with increased freshwater input. One of the specimens (Plate 3, Figure 15) displays extreme reduction of the periphragm and a rhomboidal-pentagonal endocyst with very finely perforated septa and no trace of the diagnostic galea in the dorsal view. The ecological group 'b' includes specimens from the Krajačići section in the Pannonian Basin and the Black Sea (Plate 3, Figure 16); this morphotype is considered to represent more saline conditions and it shows a galeate periphragm. Ecological group 'd' (Plate 3, Figures 6–10) contains large cysts which are interpreted as indicating development in peculiar nutrient-rich conditions as at the Maccarone Section. These diverse biometric groups were considered to have developed irrespective of the geographical realm (Paratethyan or Mediterranean) and age, with the possible exception of group 'd' which in 2009 was only recorded for the latest Messinian of the Adriatic region. However, specimens illustrated for the Lago-Mare event at the Rio Mendelin section in southwestern Spain also appear to be in this large category, with typical galeate ornament (Do Couto et al. 2014).

Most of the earlier reports of *Galeacysta etrusca* occurrences in the Pannonian Basin do not illustrate the species or they show a spherical endocyst with trellised galea in unspecified, but presumably polar view (Sütő-Szentai 2000). The first appearance is given as 8.1 Ma in a low salinity distal lacustrine basin assemblage dominated by *Spiniferites balcanicus*, after which *Galeacysta etrusca* becomes the main species at the top of the *Spiniferites balcanicus* subzone around 6.5 Ma in the central basin (Sütőné Szentai and Ildikó 2003). Later, however, Sütőné Szentai (2010) gives an age of 7.9 – 9 Ma for her late Pannonian *Galeacysta etrusca* zone which she subdivides into an older *Spiniferites virgulaeformis* Sütő 1994 and a younger *Spiniferites cruciformis* subzone. Following Bertini and Corradini (1998), she considers that *Galeacysta etrusca* is the only Pannonian Basin dinocyst which clearly emigrated out of the low salinity basin into waters of the Mediterranean region during the Lago Mare events.

For the southwestern Pannonian Basin, Bakrač et al. (2012) provide a different late Pannonian zonation and show its correlation with studies of Sütő-Szentai (1988) and Magyar et al. (1999); this *Galeacysta etrusca* zone extends from ca. 8.2 – 5.3 Ma within Martini's Nannofossil Zone NN11. The base of the zone is marked by the first occurrence (FO) of *Galeacysta etrusca* in the distal basin, and follows earlier occurrences of *Spiniferites balcanicus* back to NN9b. The distal basin *Galeacysta etrusca* assemblage is described as dominated by *Galeacysta etrusca, Spiniferites balcanicus, Spiniferites maisensis* Sütő 1994*, Spiniferites virgulaeformis* and *Spiniferites cruciformis,* but the range chart shows that the last species only appears in the latest Pannonian and becomes sporadic by the earliest Pontian interval of Piller et al. (2007) when the basin was linked to the Black and Caspian Seas. Bakrač et al. (2012) provide excellent LM images of all these taxa which co-occur at the end of the Pannonian interval. Lateral and dorsal views of Bakrač's *Galeacysta etrusca* (reproduced here in Plate 3, Figures 13, 14) show the typical galeate periphragmal features of the holotype, and endocyst shapes varying from rhomboidal to subspherical. However, one rhomboidal specimen (Bakrač et al. 2012, pl. 2, fig. 10), which

is cited as being a ventral view but actually appears to be a dorsal view, seems to have a smooth periphragm that is not clearly open along the sulcal area and thus cannot be confidently assigned to *Galeacysta etrusca*. The LM images of *Spiniferites cruciformis* (ibid pl. 2, figs. 3 and 17) show the distinctly cruciform endocyst shape and ornament of *Spiniferites cruciformis* form 1, although one specimen (fig. 17) is slightly crumpled, giving it a superficial similarity to *Pontiadinium inequicornutum* Balteş 1971. Bakrač et al. (2012) consider that *Galeacysta etrusca* is a highly effective marker for the connection and/or isolation phases of various basins adjacent to the Mediterranean and they cite the vertical distribution of *Galeacysta etrusca* at Eraclea Minoa in southern Sicily as recording a relative high sea-level and precisely demarcating the exchange between the Paratethyan Pannonian and Dacic basins, with 'primarily a one-way traffic out of Lake Pannon towards the Eastern Paratethys'.

Within the Mediterranean region, *Galeacysta etrusca* is reported from Agios Sostis at the top of a Messinian turbidite sequence (Kontopoulos et al. 1997) where it co-occurs with *Lingulodinium machaerophorum*, *Spiniferites* cf. *maisensis, Achomosphaera* and *Impagidinium* spp. In the lower Fonte dei Pulcini A section of eastern Italy, *Galeacysta etrusca* occurs in a low diversity dinocyst assemblage (Cosentino et al. 2012) interpreted as indicating a shallow oligohaline–low mesohaline (0.5–10 psu) environment with sporadic river discharge, as determined from ostracod and stable isotopic data. In Sicily, *Galeacysta etrusca* dominates the lower late Messinian Arenazzolo Formation, within an assemblage of other brackish Paratethyan taxa, including the cyst of *Pentapharsodinium dalei*, species of *Homotryblium* and *Hystrichokolpoma, Impagidinium caspienense*, *Impagidinium globosum* Sütő-Szentai 1985*, Hystrichosphaeropsis obscura* Habib 1972, '*Millioudodinium punctatum*' (Balteş 1971) Stover and Evitt 1978, (= *Cribroperidinium punctatum*?), *Lingulodinium machaerophorum, Melitasphaeridium choanophorum* (Deflandre and Cookson 1955) Harland & Hill 1979*, Pontiadinium* spp., *Operculodinium centrocarpum*, *Pyxidinopsis psilata, Spiniferites bentorii* subspp., *Polysphaeridium zoharyi* (Rossignol) Bujak et al. 1980, *Spiniferites cruciformis, Spiniferites tihanyensis* (Sütő-Szentai 2000) and *Spiniferites validus* Sütő-Szentai 1982 (Londeix et al. 2007). Here *Galeacysta etrusca* is interpreted as corresponding to a relative high-stand sea-level with oceanic influxes, low seasonal sea-surface salinity contrast and more humid climate. The brackish Paratethyan taxa in the Arenazzolo Formation were used to determine a ∂SSS index by the Mutual Climatic Range method (ibid 2007) which is primarily based on estimates of salinity from modern species distributions but is not a quantitative measure of SSS. Using this semi-quantitative index, however, *Galeacysta etrusca* corresponds to increases in salinity variation from ca. 1 – 5 psu.

Another Mediterranean site is the Rio Mendelin section in the northern Alboran Sea where Do Couto et al. (2014) describe Lago Mare deposits with respect to the Messinian Salinity Crisis. These latest Messinian – early Zanclean deposits record the first influx of Paratethyan organisms around 5.6 – 5.33 Ma, during the last two-way water exchange between the Mediterranean and the former Paratethys. The Rio Mendelin Lago Mare sediments contain ∼50% of Paratethyan dinocysts, mostly dominated by *Galeacysta etrusca* (21 – 28%), accompanied by *Pontiadinium* spp. (3 – 11%) and with fragments of *Spiniferites* spp. of brackish affinity. SEM images of the *Galeacysta etrusca* specimens (reproduced here in Plate 3, Figure 6) indicate large 'd' type cysts with well-developed galeae, atabular ventral surfaces and raised sutural ridges in the dorsal paracingular area, as in the Cava Serredi type specimens.

In the semi-marine Marmara Sea and low salinity marine Black Sea, *Galeacysta etrusca* is not present in the Holocene to recent sediments that we have studied for more than 40 core sites. The report of *Galeacysta etrusca* in the Holocene interval of core 1 of DSDP (Deep Sea Drilling Program) Site 380 (Ferguson 2012) may be erroneous because the top of drill-hole core sediments (Units 1 and 2 in piston cores) were not recovered; therefore 0 m does not represent recent time and about 6000 years of Holocene sediment deposition is missing (Stoffers et al. 1978; Ferguson et al. 2018). However, *Galeacysta etrusca* is common to sporadically present in Late Pleistocene sediments (Roberts 2012; Shumilovshikh et al. 2013) and it is abundant in lower Unit 1 (0 – 332.5 m) of DSDP Site 380 which includes organic-rich mud layers and diatomaceous sandy mud with some freshwater diatoms. DSDP Site 380 is located on the lower slope of the continental shelf north of the Bosphorus Strait where Mediterranean water enters the Black Sea during interglacial stages. SEM and LM images (Plate 3, Figures 16, 18–20) show that periphragm development is variable, including the reduced form 'b' illustrated by Popescu et al (2009, reproduced here in Plate 3, Figure 16) and forms with a typical galea as seen in lateral and dorsal views. At this site, *Galeacysta etrusca* co-occurs with stenohaline and euryhaline taxa, including *Impagidinium* sp., *Spiniferites bentorii* (Rossignol 1964) Wall & Dale 1970, *Spiniferites mirabilis* (Rossignol 1964) Sarjeant 1970, *Lingulodinium machaerophorum*, *Hystrichokolpoma* and *Achomosphaera andalousiensis* Jan du Chêne 1977 emend. Jan du Chêne & Londeix, 1988 (Ferguson 2012); however, it is most abundant in the lowest cores 8 – 5 which are interpreted as representing the interglacial substages MIS 5e (top of Core 8) to MIS 5a (top of Core 5). Here there are intervals where *Galeacysta etrusca* dominates (ca. 60 – 100%) in a low diversity assemblage with *Pyxidinopsis psilata* and *Spiniferites cruciformis*. The presence of *Lingulodinium machaerophorum* in several samples (Figure 5) indicates that the SSS was at least 8 psu (Mertens et al. 2012). In contrast to these abundances in the Late Pleistocene, Grothe et al. (2014) show that at DSDP Site 380A, only minor amounts of *Galeacysta etrusca* occurred during the late Miocene, with the first occurrence at the Maeotian/Pontian boundary (∼6.1 Ma). Specimens from contemporary Pontian sediments at Zheleznyi Rog on the Taman Peninsula (between the Azov and Black Seas) show greater abundances, with a maximum relative abundance of ∼15% just before a stratigraphic hiatus dated as ∼5.6 Ma. At Zheleznyi Rog, the large 'd'- type ecomorphotype with a rhomboidal endocyst and perforate galeate ornament is present (Plate 3, Figure 25).

Ferguson (2012) made several biometrical analyses of >1000 combined specimens of *Galeacysta etrusca* and *Spiniferites cruciformis* from DSDP Site 380 using the EN:EC parameters and statistical methods of Popescu et al. (2009). The mixture analysis of these data show that in the Black Sea, most (77%) *Galeacysta etrusca* populations fall within the marine small group 'b' and brackish group 'c' ecotypes and most *Spiniferites cruciformis* specimens overlie the boundary between the small group 'b' and brackish group 'a' ecotypes. Principal components (PC) discriminant analysis shows a consistent separation of the taxa with probability of 88.9% for *Galeacysta etrusca* and 86.2% for *Spiniferites cruciformis*, so that any specimen could be correctly identified based solely on the EN:EC measurements. The analysis also shows that *Galeacysta etrusca* consistently has a larger EN:EC ratio than *Spiniferites cruciformis* and although the species have similar 'overall size' (PC1) and length:width (L:W) ratios (PC3), on average, *Spiniferites cruciformis* has smaller EN:EC size ratios (PC2).

Although *Galeacysta etrusca* has not been found in Holocene and modern sediments at most Black Sea sites, it is occasionally present in surface and Late Pleistocene – Holocene samples of the endorheic Caspian and Aral Seas where water level and salinity are sustained entirely by the inflow of freshwater from large rivers (e.g. Volga, Emba, Syr-Darya and Amu-Darya) and $MgSO_4$ values are 3 – 4 times higher than in

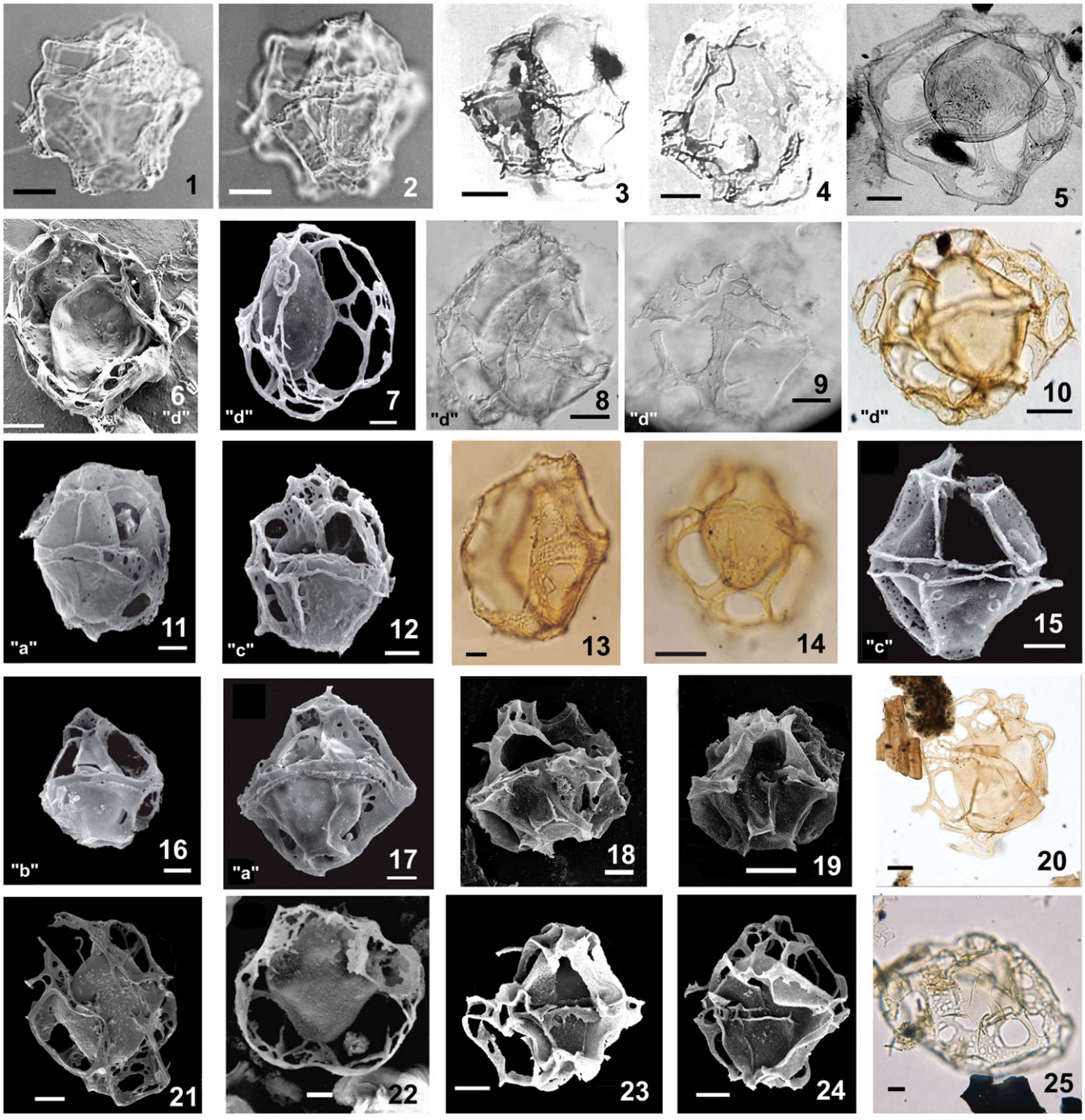

the Black Sea (Zenkevitch 1963). A specimen from the fresh-brackish water Emba Delta area of the northeastern Caspian Sea (Plate 3, Figure 16) shows the presence of prominent verrucae on the ventral surface in contrast to the psilate surface in the holotype (Plate 3, Figure 4); we also note similar verrucate ornament on specimens from deltaic settings in the Rio Mendelin and Maccarone sections of the Mediterranean region (Plate 3, Figures 6–10). Typical galeate specimens of *Galeacysta etrusca* are also present in near-surface sediment of the shallow brackish water in the northern Aral Sea (Sorrel et al. 2006, reproduced in Plate 3, Figure 22) and in Pleistocene sediment in the central Caspian Sea (Plate 3, Figures 23–24). These specimens have a scabrate ventral surface, and one Caspian Sea specimen (Plate 3, Figure 23), shows the ridged paracingular septa on the dorsal surface. Other specimens from the Volga Delta and Aral Sea are often poorly preserved and cannot always be confidently assigned to *Galeacysta etrusca* (Plate 3, Figure 5) while others have features similar to the DSDP Black Sea morphotypes (Richards et al. 2014). *Galeacysta etrusca* also co-occurs with small amounts of *Spiniferites cruciformis* and *Pterocysta cruciformis* in mid-Pleistocene sediments of the Caspian Sea, within an assemblage greatly dominated by cruciform cysts without any transitional ontological morphologies in contrast to the *Thalassiphora pelagica* assemblage at Meckelfeld, Germany (Benedek and Gocht 1981). This cruciform assemblage of probable Bakunian (mid-Pleistocene) age contains hundreds of well-preserved cruciform specimens and will be described in a separate paper. Suffice to say here, this assemblage does not include *Thalassiphora pelagica* or *Romanodinium* but it includes rare *Nematosphaeropsis bicorporis* cysts which are easily distinguishable from the other taxa.

2.4. Pterocysta cruciformis *Rochon in Rochon et al. 2003*

2.4.1. Pterocysta cruciformis *holotype and topotypes*

The last member of the '*Galeacysta etrusca* complex' to be described is *Pterocysta cruciformis* which was first observed in late Pleistocene sediment from a piston core MAR98-4 located at 112 m water depth on the Turkish Shelf of the southwest Black Sea (Rochon et al. 2003). The holotype of *Pterocysta cruciformis* is from a core depth of 130 cm which is below the latest Pleistocene α transgressive unconformity on this shelf (Aksu et al. 2002); it occurs in clayey mud with shell fragments and a coccolith flora that is dominated by *Reticulofenestra* spp. The absence of Mediterranean coccolith taxa presently found in the Black Sea suggests that the salinity was below the tolerance of most coccolithophorids (i.e. ~7 psu). These sediments probably represent the MIS 3 interstadial interval within the last glacial interval, based on mollusc radiocarbon ages of 33.15 to 44.0 ka BP (Aksu et al. 2002; Mudie, unpublished data). At this type locality, *Pterocysta cruciformis* is common and well preserved, co-occurring with common *Spiniferites cruciformis* (including all Black Sea morphotypes), *Pyxidinopsis psilata*, *Impagidinium inaequalis, Lingulodinium machaerophorum,* and the cyst of *Gonyaulax apiculata*. Although this environment was previously interpreted as a freshwater lake (Rochon et al. 2003), the presence of *Lingulodinium machaerophorum* indicates a salinity of at least 8 psu for a brackish water lacustrine environment.

Pterocysta cruciformis is a camocavate cyst with a cruciform endocyst which is characterized by the separation of the endophragm and periphragm in the sulcal area, forming a narrow, wing-like fenestrate structure over the pericoel along the central area of the ventral surface (Plate 4, Figures 3–8). The sulcal paratabulation, together with plates 1′, 4′, 1″, 6″, 1c, 6c, and 1p are expressed on the periphragm by raised ridges and perforations, with plates 1′ and 4′ possibly being fused in some specimens (Plate 4, Figures 4, 10). The ventral organization displays S-type sulcal tabulation in which apical plate 4′ or its homologue (*4′) tends to be long, predominantly ventral, and in contact with the anterior sulcal plate (as) as reflected in the perforated "wing" covering the sulcal area. The holotype is also distinguished by its relatively small size (endocyst L = 51μm; W = 48 μm) and strongly

Plate 3. SEM and LM images of *Galeacysta etrusca* and similar Paratethyan cysts with reduced ornament reproduced from Popescu et al. (2009, here as Figures 11, 12, 15 – 17). Figures 3 and 4 of the holotype are reproduced from Corradini and Biffi (1988). Scale bar = 20 μm. 'a', 'b', 'c' and 'd' indicate ecotypes from Popescu et al. (2009) Figures 1 – 4 and 6 – 10 are specimens from Mediterranean areas; Figures 11 – 15 are biometrical group 'a' and 'c' specimens from the Pannonian basin and Maccarone Lago-Mare bed; Figures 16 – 20 are biometrical group 'b' specimens and Figures 5, 20 – 25 are from Caspian and Aral Sea endorheic basins. 1 – 2. LM images of holotype from 35 mm photographic slide, showing posterior-lateral view, mid focus (1) and high focus (2). 3. LM of paratype in left lateral view. 4. LM of paratype in ventral surface view, showing the atabulate ventral surface and surrounding galeate ectocyst. 5. Specimen from Kirmaky Valley, Azerbaijan (early Pliocene); ventral view showing attachment of ectophragm on dorsal surface. 6. SEM of specimen from Rio Mendelin, Spain Lago-Mare bed, showing ventral surface and lateral galeate ectocyst ornament (from Do Soto et al. 2015). 7. SEM of specimen from Maccarone Lago-Mare sediment; ventro-lateral view showing typical atabulate ventral surface and galeate ornament (from Popescu et al. 2009). Figures 8 – 9: LMs of specimens from Lago Mare interval in the Maccarone section. 8. lateral view of specimen, showing the elliptical endocyst and perforate galea in mid view. 9. dorsal view of specimen in high focus, showing details of galea structure and attachment. 10. Optical section of specimen from Northern Appenines Lago-Mare sediment (from Adele Bertini). 11. SEM of biometrical ecotype 'a' specimen of Popescu et al. (2009) from the Krašić site in the Paratethyan basin; dorsolateral view of elliptical endocyst with attached operculum and ridged, perforate galea. 12. SEM of biometrical group 'c' cyst from the Majs 2 site in the Pannonian basin (from Popescu et al. 2009) in lateral view showing reduced galea width but prominent paracingular ridges. Figures 13 – 14 are Pannonian basin LMs of *Galeacysta etrusca* from Bakrač et al. (2012). 13. Lateral view showing the typical galeate periphragmal features like that of the holotype, and rhomboidal endocyst. 14. Dorsal view of specimen with subspherical endocyst. 15. SEM of group 'c' cyst from the Majs 2 site in the Pannonian basin (from Popescu et al. 2009), showing a dorsal view of a rhomboidal cyst with highly reduced ornament. 16. SEM showing a lateral view of an ovate group 'b' specimen from DSDP Site 380A in the Black Sea (from Popescu et al. 2009). 17. SEM of biometrical ecotype 'a' specimen of Popescu et al. (2009) from Maccarone Lago-Mare site, with features similar to the holotype; dorsal lateral view of elliptical endocyst with ridged and perforate galea. Figures 18 – 20: Specimens from DSDP Site 380, Black Sea. 18. Dorsal view of well-developed ornament. 19. Dorsal view of specimen with wide paracingular septa but reduced galea. 20. LM showing lateral view of a rhomboidal cyst. 21. SEM showing ventral view of specimen from Emba Delta core CDSE12 (late Pleistocene), N-E Caspian Sea. 22. SEM showing ventral surface of Aral Sea specimen (from Sorrel et al. 2006, fig. 10-6, mistakenly labelled as *Spiniferites cruciformis*; Sorrel, pers. comm. June 2015). Figures 23 – 24: SEMs of mid-Pleistocene (Bakunian) specimens from central Caspian Sea, showing dorsal surfaces and attached widely fenestrate galea. 23. Specimen with? microgranulate to gemmate endophragm and ectophragm surfaces. 24. Specimen with scabrate ectophragm surface. 25. LM of specimen from Pliocene sediment at Zheleznyi Rog on the Taman Peninsula, in dorsal view (provided by Arjen Grothe). SEM images of SF (18 – 19 and AR (21, 23 – 24); LM images of PJM (1, 2, 8 – 9), KR (5), SF (20), and Adele Bertini (10).

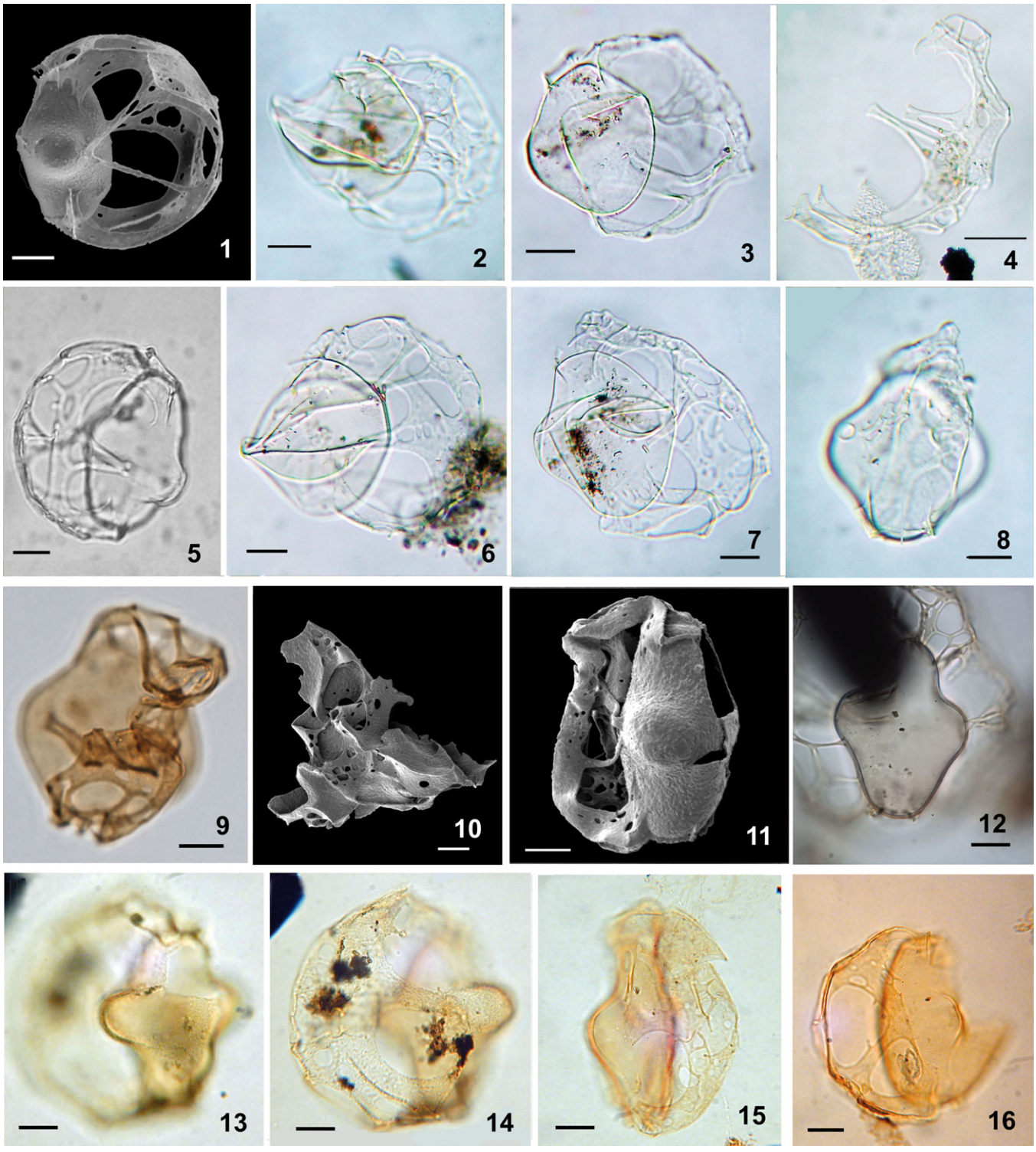

Plate 4. SEM and LM images of *Pterocysta cruciformis* from the Ponto-Caspian Seas. Scale bar = 10 μm. Figures 1 – 8: LM topotype images from core MAR 98-4, 130 cm. Figure 9: Specimen from DSDP Site 380 MIS 5a. Figures 10 – 16: Specimens from Caspian Sea. 1. SEM of specimen in lateral view showing details of ventral attachment and ectophragm structures. 2 and 3. Right lateral views of two different specimens showing the narrow ventral pterate ectocyst. 4. Lateral view of detached ectocyst. 5. Left latero-ventral view of typical strongly cruciform pterate specimen. 6. Right lateral view of a damaged cyst which appears to be wider than other topotypes. 7. Left lateral view of another less compressed cyst with folds in the dorsal and lateral paracingular areas. 8. Ventral view of 'wing' surface on a cruciform endocyst. 9. LM image from DSDP Site 380, 50.52m core depth: ventral view with focus on 'wing' surface. 10. SEM of detached ectocyst from Emba Delta surface sample, core CDSE12, 0 cm). 11. SEM of typical specimen from Emba Delta area of Caspian Sea. 12. LM of a cruciform specimen from the southern Caspian Sea identified as *Pterocysta cruciformis* by Leroy (personal communication 2015), with the dorsal surface in mid-view, showing an atypically wide ectophragm. Figures 13 – 16: LM images from surface and Holocene sediments, Damchik region, Volga Delta, showing high (13) and median focus (14) on specimen in dorso-left lateral and ventro-lateral views, and median focus views of two other specimens (15 left lateral, and 16 right lateral views). LM images of PJM (1 – 8), SF (9), KR (13 – 16), and SEM images of AR.

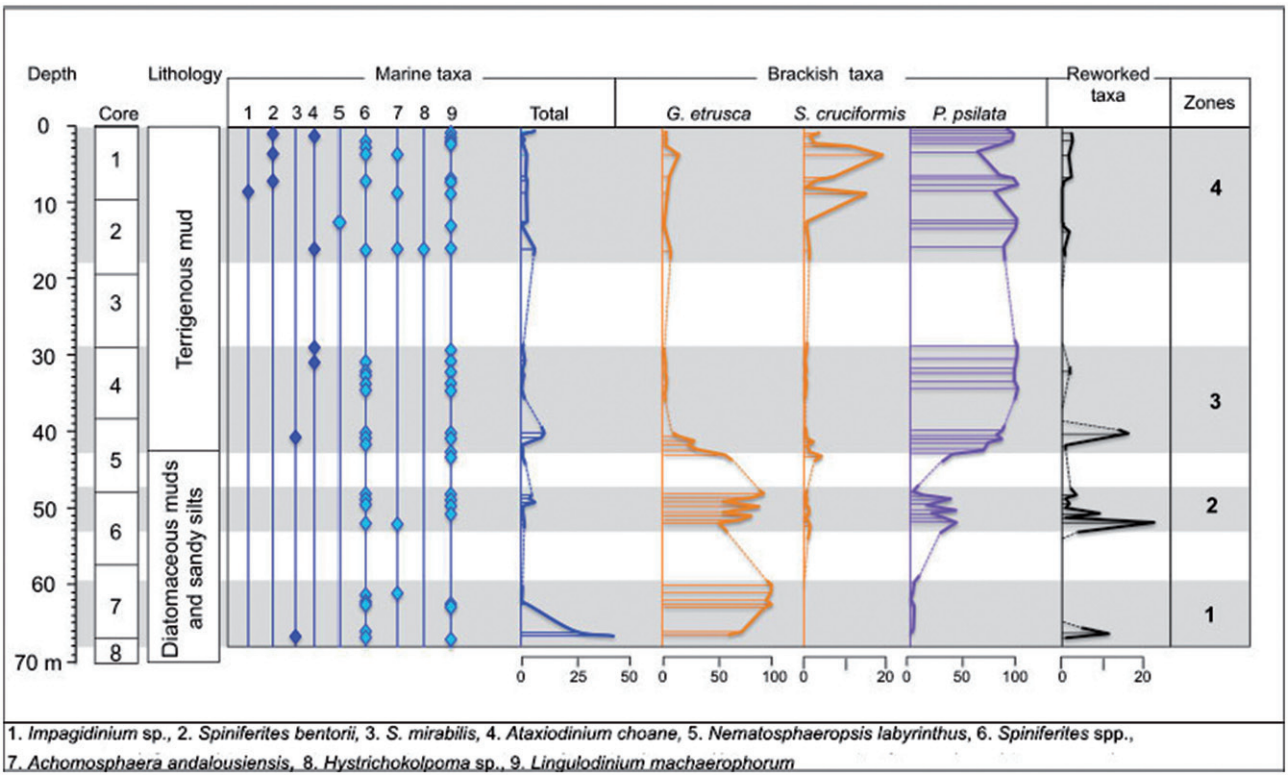

Figure 5. DSDP Site 380 cores 1 – 8 showing the distribution of nine typically marine taxa listed at the diagram base, and relative abundances of *Galeacysta etrusca, Spiniferites cruciformis* and *Pyxidinopsis psilata* as % total dinoflagellates (modified from Ferguson 2012). Zones 1 – 4 are informal palynological assemblage zones based on presence/abundance of marine or freshwater taxa.

cruciform endocyst which has well-rounded polar areas as seen in dorsal and polar views (see SEM of topotype in Figure 1.3 and LMs in Plate 4, Figures 1,5,8). This typical cruciform endocyst surface is also strongly compressed, with a width:thickness ratio of 1.12 – 1.2. The endocyst surface is shagreenate to verrucate, sometimes with additional minute (1 μm) random projections.

In apical view, the equatorial area appears broadly oval with a slightly smaller rounded polar area from which the fenestrate ectocyst separates over the ventral surface, forming a "wing" in the ventral direction (Plate 4, Figures 2, 3, 6 and Rochon et al. 2003, pl. 2, fig. 3). This feature gives the cyst the appearance of a winged 'flying saucer' or a parachute. The characteristic narrow (26 microns) wing-like fenestrate ectophragm is attached ventro-laterally in the equatorial and polar regions so that it covers only the central half to two-thirds of the ventral endocyst surface which is atabulate (Figure 1.6; Plate 4, Figures 9, 11). This pterate wing superficially resembles the galea of *Galeacysta etrusca* but it is actually the inverse of a galea because, like the protective perforated mask on a traditional fencing helmet, the pterate wing covers the central sulcal area which is wide open between the ventral edges of a *Galeacysta*-type 'helmet'. SEM images of the holotype dorsal surface (Rochon et al. 2003, pl. 2) and other specimens (Plate 4, Figures 5, 11, 13, 16) show almost no trace of cingular ornament, and there are just a few sutural traces in the apical and antapical areas in contrast to the heavily, sometimes septate dorsal surface of *Galeacysta etrusca*. The fenestrate ectophragm is attached to the endocyst at apex, antapex and the cingular area, probably at the junction between plates 1c–2c, and 5c–6c. The sulcal tabulation, together with plates 1′, 4′, 1″, 6″, 1c, 6c, and 1p are expressed on the ecotophragm by raised ridges and perforations, with plates 1′ and 4′ possibly being fused in some specimens. The cyst is relatively fragile and often there are detached ectophragmal 'wings' and endocysts with strongly reduced ornament in the same samples as the normal cysts (Plate 4, Figures 1, 4, 10). The apterate endocysts *of Pterocysta cruciformis* may closely resemble cruciform specimens of *Spiniferites cruciformis* form 5 but they are smaller and lack traces of cingular septa and sulcal tabulation other than short broken periphragm attachment features.

2.4.2. Pterocysta cruciformis *in the Ponto-Caspian Basin*

In Marmara Sea*, Pterocysta cruciformis* is also common in the Late Glacial interval (ca. 12 – 15 ka BP) of Core MAR98-12 in the central basin where it is present in low numbers within an assemblage dominated by *Spiniferites cruciformis* and *Pyxidinopsis psilata,* with rare specimens of *Lingulodinium machaerophorum, Impagidinium inaequalis* and *Achomosphaera argesensis* Demetresçu 1989 (Rochon et al. 2003). The presence of common *Pediastrum* coenobia indicate high influx of fresh water to a brackish, probably lacustrine but not freshwater environment. The species is also recorded by Londeix et al. (2009) for a neighbouring site. Elsewhere in Marmara Sea, however, *Pterocysta cruciformis* is rare and poorly preserved in late Pleistocene sediments.

In the Black Sea deep basins, *Pterocysta cruciformis* is rare in glacial stage intervals at DSDP Site 380 on the western lower slope (Ferguson 2012; Plate 4, Figure 16) and it is occasionally present in the interval between Eemian and glacial stage sediments of cores from the southeastern Black Sea basin (Shumilovskikh et al. 2013 and personal communication August 2015).

In the northern Caspian Sea, where salinity is low and sea-ice covers the surface from November to March (Kosarev and Yablonskaya 1994), *Pterocysta cruciformis* is present in low numbers in the Volga Delta region (Richards et al. 2014a), in surface sediments (Plate 4, Figures 13–14) and in cores of Holocene age (Plate 4, Figures 15–16). *Pterocysta cruciformis* is also locally common in late Pleistocene sediments in the Emba Delta region (northeastern Caspian Sea) and consistently present in low numbers in the offshore central Caspian region in mid-late Pleistocene sediments (Richards 2014b). It is reportedly discontinuously present in late glacial to early Holocene sediments of the central and southern basins (Leroy, personal communication, September 2015), but some of these southern forms have unusually wide periphragms (Plate 4, Figure 12) and more study is needed to confirm their identity. The species has not been reported for the Aral Sea.

3. Other taxa in the '*Galeacysta etrusca* complex'

Popescu et al. (2009) consider that the galeate parachute and cruciform taxa from Miocene – Pliocene Mediterranean and Paratethyan sediments include morphologies that are transitional between the species *Galeacysta etrusca, Nematosphaeropsis bicorporis, Romanodinium areolatum* and *Spiniferites balcanicus*. Hence they suggest that all these taxa are variants of a single species which they called the *Galeacysta etrusca* complex and they consider that the taxa differ only in degree of expression of tabulation and pericoel [sic] development. They further note that the name *Romanodinium areolatum* would take precedence for this complex if it was validated. This onto-morphological and phenotypical interpretation is essentially the same as that proposed by Benedek and Gocht (1981) for morphotypes of *Thalassiphora pelagica* from core 149-152 of the Meckelfeld-86 borehole near Hamburg, Germany.

In historical sequence of their recognition, the first species of Popescu's *Galeacysta etrusca* complex is the large (up to 85 μm total width) apparently camocavate to circumcavate species *Romanodinium areolatum* which is moderately abundant in late Miocene/earliest Pliocene (Pontian Stage) deposits of Romania. The holotype (Slide L.C. 8992 -60/118) is described as having an essentially rounded endocyst without tabulation, and a thin hyaline outer cover, with rare longitudinal folds, and an apical aperture/pylome with irregular edges. The antapical wide transparent 'non-homogeneous' membrane is perforate in some specimens and has a scalloped appearance (Balteş 1971). Unfortunately, the holotype was not designated and the type illustrations were erroneously cited as Balteş 1971, pl. 5, fig. 1, 2 which are in fact images of a proximate *Chytroeisphaeridia* sp. However, in pl. 3, fig. 1 – 2, Balteş provides LMs of two specimens cited as *Romanodinium areolatum* gen. nov., sp. nov. in the plate caption. When rotated 90° clockwise, these specimens appear similar to forms of *Thalassiphora pelagica* described by Eaton (1975-1976, p. 286 – 287). *Thalassiphora pelagica* has a slightly dorso-ventrally compressed endocyst and a spongy fibrillar periphragm that is separated from the endophragm by a distinct pericoel except over the mid-dorsal surface (Plate 5, Figures 16–19). This inflated periphragm development style in a different plane is also found in the lower – mid Miocene taxon *Cousteaudinium aubryae* de Verteuil and Norris 1996 which is recorded for the central Paratethyan basin during the Langhian stage (Bakrač et al. 2012, pl. 1, fig. 32); notably, *Cousteaudinium aubryae* also has a rounded apical archeopyle. It seems that the periphragm of *Romanodinium areolatum* is basically formed in the same way as these two cribroperidinioidean taxa (*sensu* de Verteuil and Norris 1996), and in the fossil dinocyst classification of Norris (1978), *Romanodinium* and *Thalassiphora* are grouped together in the subfamily Thalassiphoroideae. However, de Verteuil and Norris (1996) consider that *Cousteaudinium* is both circumcavate and variably chorate, based on the presence of hollow, tubular processes in some morphotypes.

The absence of a holotype designation for *Romanodinium areolatum* and the limited holotype description means that the gonyaulacalean affinity of *Romanodinium* is presently uncertain. However, there is no basis for assigning the species to either *Spiniferites* or *Galeacysta* because it clearly differs from these taxa in periphragm structure, style of pericoel development, tabulation, and absence of any solid processes. Further studies of Recent specimens identified by various authors as *Romanodinium areolatum* or cf. *Thalassiphora* from Caspian and Aral Seas (Plate 5, Figure 2, and Sorrel et al. 2006 figs. 8, 1–5) are needed to clarify the morphology and gonyaulacalean affinity of *Romanodinium areolatum* and relate this taxon to the three key Paratethyan marker species of the *Galeacysta etrusca* complex. For example, a SEM image of a Tortonian specimen of *Romanodinium areolatum* from the Maj 2 site in the Pannonian Basin and fluorescent microscope images from DSDP Site 380A (in Suc et al. 2015, pl. 1, fig. 5) show left ventro-lateral views of a large cyst with an apparently rhomboidal endocyst lacking paratabulation on the lateral and dorsal surfaces, and with densely micro-perforate pterate structure and a single fenestrate opening in the epicystal area. The SEM image very closely resembles cysts called *Spiniferites balcanicus* by Bakrač et al. (2012), which is reproduced here in Plate 5, Figure 8. Other sub-rounded specimens from late glacial sediment of Marmara Sea core MAR02-98P (Plate 5, Figure 1) and MAR 94-5 (Plate 5, Figures 13–15) may also be specimens of *Romanodinium areolatum* but with light microscopy, they cannot clearly be distinguished from *Thalassiphora 'subreticulata'* of Fensome and Williams (2004; species not yet validly published) and the *Invertocysta* species A and B of Londeix et al. (2009, pl. III, figs. 7 and 10).

Another large (length = 120 – 130 μm) camocavate taxon which is abundant in the upper-Miocene/lower Pliocene

deposits of the Pannonian basin is *Thalassiphora balcanica* Balteş 1971 which was subsequently emended and re-combined as *Spiniferites balcanicus* (Balteş) Sütő-Szentai 2000. Balteş (1971) describes *Thalassiphora balcanica* as a pterate cyst with an ellipsoidal central body partly enfolded in a membranous periphragm forming a 'lamellate wing' which is in contact with the endophragm only on one side (presumed the dorsal side). The membrane is described as fibrous and of quasi-reticulate appearance, with perforations. The cyst has a wide trapezoidal precingular archeopyle and vaguely outlined cingulum but otherwise lacks paratabulation. These features are evident on the LM image of the holotype (designated by Sütő-Szentai 2000 as Balteş 1971, pl. 3, fig. 3) and three topotypes (Balteş 1971, pl. 3, figs. 4-6). However, one image (ibid, pl. 3, fig. 7) shows a lateral view of a cyst with a fenestrate periphragm more similar to that of *Galeacysta*.

For the same reason as *Romanodinium areolatum*, *Thalassiphora baltica* is also not a valid name. It was considered to be a junior synonym for *Thalassiphora (Pterosperma) pelagica* according to Stover and Evitt (1978) and by Fensome and Williams (2004). Sütő-Szentai (1988, pl. IV, figure 2) attempted (invalidly) to transfer *Thalassiphora baltica* to *Spiniferites* and she provided a LM of *Spiniferites balcanica* comb. nov. from upper Pannonian deposits in the Bácsalmás No 1 borehole (433 – 438 m). This image presents a lateral view very similar to the typical *Spiniferites balcanicus* specimen of Bakrač et al. (2012). In contrast, in a second attempt (also invalid), she published two other LM images of *Spiniferites balcanicus* comb. nov from the Majs borehole, 204.7 – 204.8 m (as Sütő Zoltánné 1994, pl. V and VI). These 1994 images are very different from that of the 1988 publication: one has highly reduced, undecipherable ornament (Sütő Zoltánné 1994, pl. V) and the other has a fenestrate periphragm and attachments like those of *Galeacysta etrusca* (ibid pl. 6). In this same paper, a ventral view of a typical *Galeacysta etrusca* specimen (ibid, pl. VII) is shown and is presented as a separate species that is considered to be a planktonic (thecate) dinoflagellate form.

The emended diagnosis of *Spiniferites balcanicus* describes an ovoidal or spheroidal body with two membranes 'fixed both on the right and left side of the sulcus' and sometimes with two wing-like membranes that are 'differently perforated', one of them being arched in the apical area and being partially connected except in the ventral area. However, LM images of three specimens from the Paks 4 borehole (Sütő-Szentai 2000, pl. IX figs. 1-3) neither demonstrate these features clearly nor support the differential diagnosis which distinguishes *Spiniferites balcanicus* from *Subathua balcanica* (Balteş) Khanna and Singh 1980 (an invalid name), *Thalassiphora* (Eisenack) Eisenack and Gocht 1960, and *Galeacysta etrusca* based on adhesion of membranes, tabulation formula and 'threefold division of the processes'. Sütő-Szentai's amendment ends with the closing remark that *Thalassiphora pelagica*, *Galeacysta etrusca* and *Spiniferites balcanicus* all bear similar membranes, development of which '… during their life cycle could be controlled by similar functional purposes responding to similar ecological conditions' (Sütő-Szentai 2000, p. 164). This ecological response idea may be essentially correct (see Section 4) but the ontology and structure of the 'membranes' (presumably referring to the periphragm) appears to be dissimilar in several features: origin from the cyst wall, internal structure, attachment points and the reflected tabulation which is clearly expressed in the claustra and ridges on the galea of *Galeacysta etrusca* but is very weakly expressed on the periphragms of *Thalassiphora pelagica* and *Spiniferites balcanicus* as described by Balteş (1971). Given that expression of basic paratabulation remains a consistent feature within the morphologically and ecologically highly variable species *Spiniferites cruciformis* (Sect. 2.2), it seems unlikely that environmental plasticity could account for blurring of the tabulation and periphragmal textural characteristics that distinguish the three key species in the '*Galeacysta etrusca* complex'.

Spiniferites balcanicus cysts from deposits of probable Pliocene age in the Zheleznyi Rog section on the Taman Peninsula appear to be remarkably similar to the Palaeocene species *Thalassiphora 'subreticulata'* (Plate 5, Figures 6–7) according to Fensome & Williams (personal communication, 2015), and they differ from *Thalassiphora pelagica* morphotypes in Caspian and Taman samples (Plate 5, Figures 16–17, respectively) in having a visibly less dense periphragm composition which gives the wing in *Thalassiphora pelagica* a more solid (minutely lacunate) appearance, and in not having the characteristic 'attachment appendage' of *Thalassiphora pelagica* morphotype D, the purported floating cyst stage of Benedek and Gocht (1981). *Spiniferites balcanicus* is also much larger than the three core species of the '*Galeacysta etrusca* complex' and no intergrades between the taxa have been described, so it is not possible to demonstrate a morphological gradation with *Galeacysta etrusca*. Black Sea and Taman peninsula cysts (Plate 5, Figures 3–5, 9 – 11) also differ from the *Spiniferites balcanicus* image of Bakrač et al. (2012, reproduced here as Plate 5, Figure 8) in that they show well-defined dorsal paracingular tabulation whereas the Pannonian cyst lacks these features. An SEM image of *Spiniferites balcanicus* in Suc et al. (2015, pl. 1, fig. 3) however, shows a galeate cyst with an atabulate ventral surface which closely resembles the ventral view of the *Galeacysta etrusca* holotype. In the same paper, *Galeacysta etrusca* is illustrated by an SEM in dorsal view, showing the typical ridged dorsal paracingular features (ibid pl. 1, fig. 1). None of these specimens have a cruciform endocyst.

The late Pannonian species *Nematosphaeropsis bicorporis* by Sütő-Szentai (1990) is not a validly published name because the holotype location is not specified and in 1989, Sütőné Szentai (1989, pl. 6, fig. 3) did not provide a description. The holotype looks like *Galeacysta etrusca* but other specimens more closely resemble *Seriliodinium explicatum* (Plate 5, Figure 12). However, the endocyst is oval-rhomboid, not cruciform and it is doubtful that this taxon can be linked to morphotypes of *Seriliodinium explicatum* or *Spiniferites cruciformis* form 1 with single trabecula strands.

Pterocysta cruciformis is superficially similar to the Miocene species *Lophocysta sulcolimbata* Manum 1979 but that taxon has an ovoid endocyst and L-type ventral organization, with a ribbed crest of fibrous texture. Rochon et al.

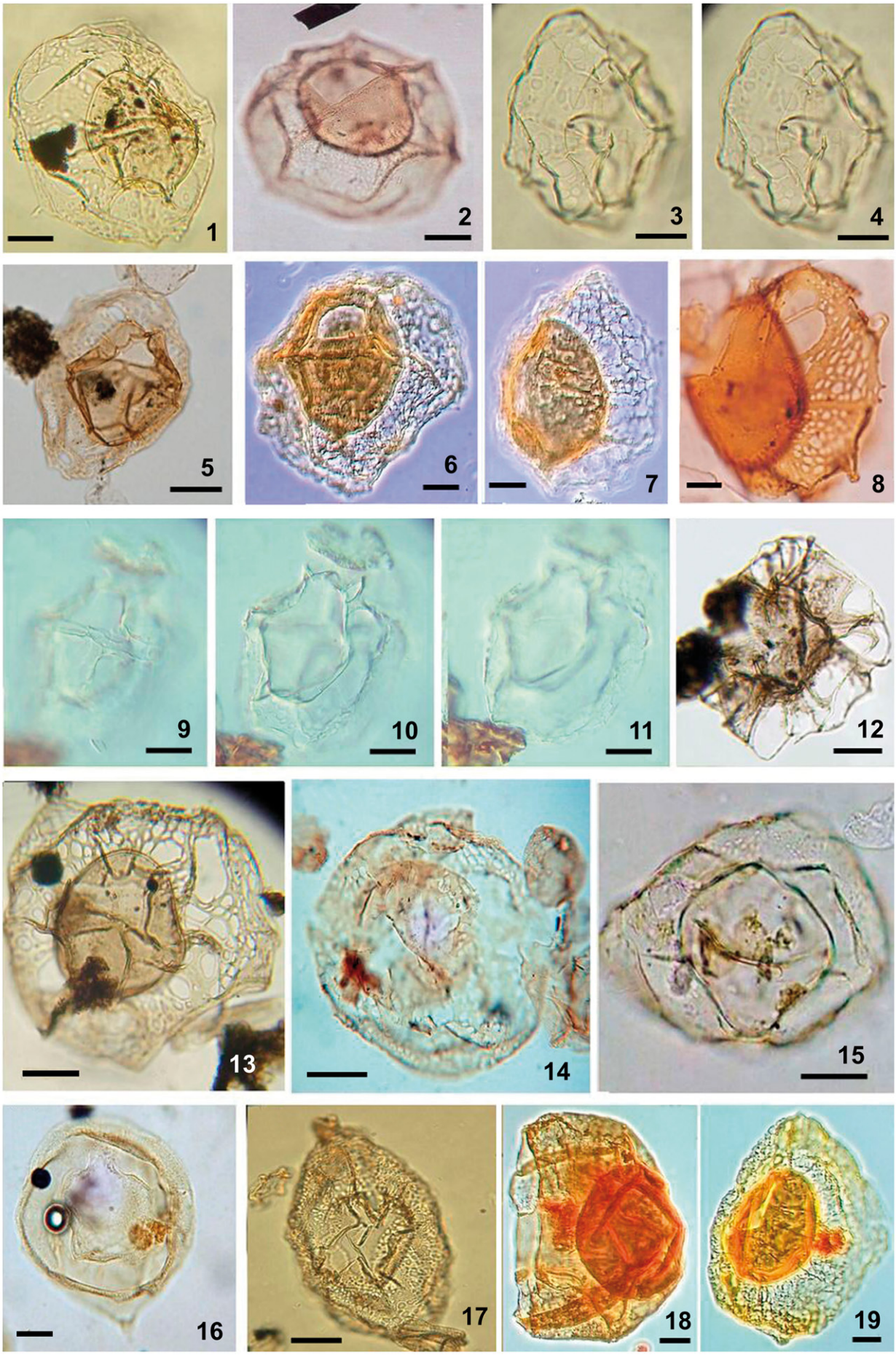
1
2
3
4
5
6
7
8
9
10
11
12
13
14
15
16
17
18
19

(2003) provide other comparisons with cruciform and camocavate gonyaulacoid taxa to highlight several inter- generic differences, as also summarised here in Table 2, including the small Neogene Mediterranean species *Piccoladinium fenestratum* of Versteegh and Zevenboom (1995).

Exclusion of these four of the six taxa in the proposed *Galeacysta etrusca* complex on the basis of morphological features and/or incomplete species delimitation leaves only *Galeacysta etrusca* and *Spiniferites cruciformis* within the 'complex'. We have shown that the holotype of *Galeacysta etrusca* differs from *Spiniferites cruciformis* and other genera in multiple characteristics, primarily as a result of their basic camocavate versus chorate cyst forms. It appears that the suggested intergradations (Popescu et al. 2009 and references therein) of these taxa is largely an artefact of focussing on the use of morphometrical EN:EC ratios as a primary parameter for distinguishing between the taxa. The EN:EC ratios can show a size continuum in space and time but it does not follow that this indicates a merging of three genera that differ in basic wall structure and in multiple ectophragmal features.

4. Stratigraphic ranges and evolutionary trends.

It appears that although morphometrical studies of the so-called '*Galeacysta etrusca* complex' can be useful in pointing to palaeosalinity affiliation, the apparent intergradation of morphotypes over intervals of thousand to millions of years is an illusion that can confuse species recognition and mask useful marker species ranges in the Black Sea and other marginal Mediterranean seas. For example, at DSDP site 380, Ferguson (2012) found an effective replacement of the larger rhomboidal galeate *Galeacysta etrusca* by the smaller cruciform *Spiniferites cruciformis* which is rarely present at this site before the end of MIS 2 (Figure 5, upper Palynological Zone 4, and Ferguson et al. in press). Using new data from other Black Sea cores (Aksu et al. 2002; Shumilovskikh et al. 2014), we can now trace the range of *Pterocysta cruciformis* to MIS 5, and this reveals a succession of acmes, from the large galeate, rhomboidal *Galeacysta etrusca* in the warm early Eemian, to the small cruciform, winged *Pterocysta* during the glacial stages and MIS 3, followed by an acme of *Spiniferites cruciformis* in late MIS 2 to early Holocene. New data from the Caspian Sea also extend the range of common *Pterocysta cruciformis* to within the late Pleistocene (MIS 3) and there are rare to consistent occurrences of *Pterocysta cruciformis* at least down to the mid-Pleistocene (Richards et al. 2014b and this paper, Figure 6).

In final summation, it seems that although morphometrical studies of the *Galeacysta etrusca* complex can be useful in pointing to general palaeosalinity affiliation and that EN:EC statistics can reveal a size gradient, the apparent overlapping of biometrically defined morphotypes masks useful differences in the marker species ranges and acmes. Rochon et al. (2003, p.102) noted that 'the apparently explosive appearances in the Late Pleistocene of gonyaulacacean species with cruciform cyst bodies raise important (although unresolved) questions about the possible evolution of this shape in low salinity environments that are periodically isolated by emergent sills during glacial low sea-level stands'. They also noted that the earliest subcruciform (biconical) morphotype was *Achomosphaera argesensis* which appeared at the end of the separation of the Baltic–Pontian–Black Paratethyan basins, concurrent with their isolation from the Mediterranean between ca. 19 and 8 Ma. This event was followed by the appearance of *Seriliodinium explicatum* in the Black Sea and *Spiniferites cruciformis* in the Mediterranean Sea, followed by *Pterocysta* and cruciform cysts of *Pyxidinopsis psilata* in the Black Sea.

Here we show a new possible evolutionary series (Figure 6) commencing with the Palaeogene taxon *Thalassiphora balcanica* taken as synonymous with *Thalassiphora pelagica* and/or *Thalassiphora 'subreticulata'*. Unfortunately, it has not been possible to locate the holotype of *Achomosphaera argesensis* or topotypes from the Arges type locality in Romania, so we cannot provide further first-hand information on this ovoidal-biconical taxon. However, Vladimir Torres (2nd Spiniferites Workshop, July 2015) reports that new photographs indicate this atabular *Achomosphaera* species is distinguished by membranes connecting the apical gonal processes of this chorate cyst. We also consider that *Seriliodinium explicatum* is a probably trabeculate morphotype of *Spiniferites cruciformis* form 1 that can display a large degree of phenotypic plasticity as found in cysts of the *Gonyaulax spinifera* 'complex' (Rochon et al. 2009) and we do not show the presumed Plio-Pleistocene genus *Seriliodinium* in the chart. Our chrono-morphological

Plate 5. LM images of camocavate to circumcavate cysts from the Ponto-Caspian Seas, *Thalassiphora pelagica* and *Thalassiphora 'subreticulata'* from the Nova Scotian Shelf (Figures 6, 7, 18, 19), and *Seriliodinium explicatum* from Black Sea (Figure 12). Scale bar = 20 μm. 1. *Thalassiphora* sp. specimen from late Pleistocene interval in Marmara Sea core MAR02-89P, 590 cm. 2. Dorsal surface of cf. *Thalassiphora* from Kara-Bogaz Gol, Caspian Sea late Holocene (image of SAG Leroy; see also Leroy 2010). Figures 3 – 4: Dorso-lateral views of *Spiniferites balcanicus* specimen with cruciform endocyst from Marmara Sea late Pleistocene sediment in MAR012-89P, 540 cm, showing mid focus (3) and high focus (4). 5. Dorsal view of cf. *Galeacysta etrusca* specimen with perforate fenestrate ectophragm from DSDP Site 380, 60 m. Figures 6 – 7: Video-capture images of two specimens of *Thalassiphora 'subreticulata'* of probable Eocene age, showing dorsal (6) and right lateral (7) views. 8. Specimen of *Spiniferites balcanicus* from Pannonian Sea, in right lateral view and showing the perforate ectophragm with fenestrate opening in the apical area (from Bakrač et al. 2012). Figures 9 – 11: cf. *Spiniferites balcanicus* specimen from Section TM 11 on the Taman Peninsula, with age of ~5.7 Ma, in high (9), mid (10) and low (11) focal views. 12. Specimen of *Seriliodinium explicatum* from late Pleistocene sediment, Marmara Sea core MAR02-89P, 260 cm, in optical section. 13. Specimen of cf. *Thalassiphora pelagica*, SW Black Sea early Holocene of MAR05-13P, 790cm, in optical section. 14. Specimen of cf. *Thalassiphora pelagica* from an outcrop of Kirmaky Suite (early Pliocene), Azerbaijan, western Caspian Sea, in optical section. 15. Specimen of cf. *Thalassiphora pelagica* from Marmara Sea core MAR02-89P late Pleistocene sediment, in high focus on dorsal surface. Figures 16 – 17: Specimens of *Thalassiphora pelagica* from Taman peninsula Pliocene sediments, showing the typical spongy-textured periphragm and V-shaped attachment structure (16) and finely-lacunate fibrous texture, lacking claustra and vesicular openings (17). Figures 18 – 19: Video-capture images of two specimens of *Thalassiphora pelagica* in right (18) and left (19) dorso-lateral views, Scotian Shelf Shubenacadie Well sample of RA Fensome. LM images mostly by PJM except as noted: (2) from Suzanne Leroy, 16 – 17 from Arjen Grothe, (5) SF, (14) KR, and video-capture images 6 – 7, 16 – 17 from RA Fensome.

Table 2. Comparison of salient, easily visible features of cruciform, 'pterate' and galeate taxa and their endocyst dimensions. Dimensions are for dorsal view: L = length; W = width, D = thickness. M = medium; VL = large; S = small

Taxon	Endocyst shape	Endocyst Parasuture	Ectophragm/Periphragm	Periphragm attachment	Endocyst Size LxWxD μm
Romanodinium areolatum	Subsphaerical	Atabular	Camocavate; spongy, fibrous, hyaline periphragm, +/- perforate covers the hypothecal pericoel	Paracingular	M 50x45 – 60x48
Spiniferites balcanicus/ Thalassiphora balcanica	Ellipsoidal	Faint para-sutures	Camocavate cyst, fibrous, reticulately perforate membrane with ventral opening	Dorsal	VL 100x90x90
Galeacysta etrusca	Ellipsoidal, straight sides	Yes, strong, with raised dorsolateral cingular ridges	Claustrate – fenestrate ventro-lateral galea with open atabular sulcal area	Dorsal; membranes or rods	M 66x52x60 [W = 45(52)58]
Achomosphaera argesensis	Ovoidal-biconical	No	Fenestrate solid processes	N/A	M 48x35x34
Spiniferites cruciformis	Cruciform, downward concave sides; rarely pyriform; always strongly compressed	Yes, all surfaces	Parasutural membranes supported by broad processes of varied length, fine-perforate; rarely trabeculate	Parasulcal septa, gonal processes & lateral para-sutures, varied length	M 46-65 x 34-56 x28
Seriliodinium explicatum	Cruciform/biconical to oval; compressed	Yes	Parasutural membranes linked by trabeculate process ends, appearing fenestrate	Lateral parasutures & processes	M 48x39x?(nd)
Pterocysta cruciformis	Cruciform/biconical; compressed	No	Narrow penitabulate ventral (sulcal area) pterate crest	Ventral	S 46x41x29
Lophocysta sulcolimbata	Ovoidal	No	Cavate, almost covered by reticulate periphragm	Ventral	S 48x38x35
Piccoladinium fenestratum	Ovoidal	No	Camocavate, with enveloping penitabulate periphragm and large intra-paraplate holes	Dorsal	S 22-27x17-27

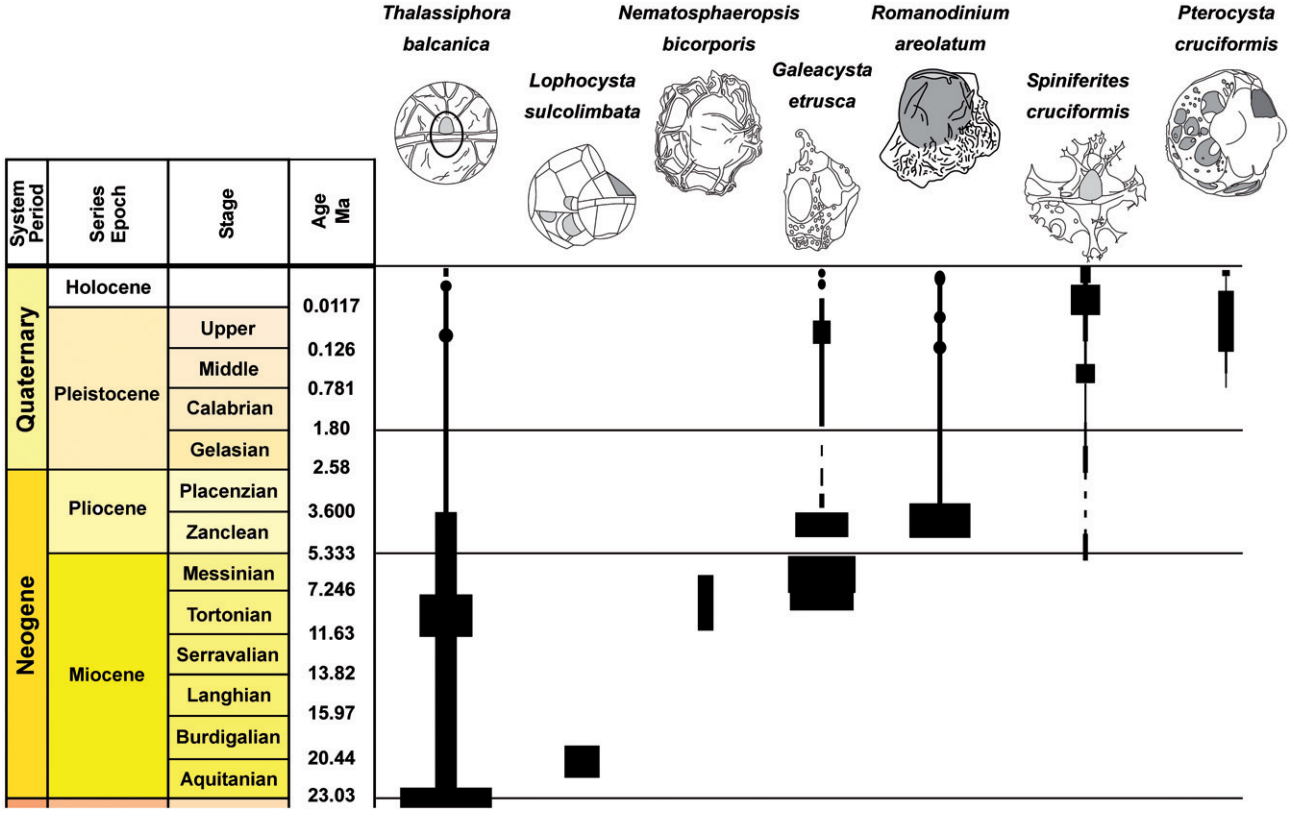

Figure 6. Probable stratigraphic ranges of members of the "*Galeacysta cruciformis* complex" according to the geological timescale of Cohen et al. (2013). The age of the Pleistocene – Holocene boundary (MIS2/1 boundary) is almost the same as that given by Lewis and Maslin (2015). The base of MIS 5 is at the Middle – Upper Pleistocene boundary. Line drawings of taxa are either from Graham Williams and Bill MacMillan (with kind permission) or were made by André Rochon (*Spiniferites* and *Pterocysta*).

scheme suggests there is a successive reduction in endocyst size and ectophragm expansion, perhaps reflecting increasing economy of growth energy as might be expected to accompany a progressively cooling Plio-Pleistocene climate, and culminating in the maximum reduction evident in *Pterocysta cruciformis*. Similar observations have been made by Sarjeant et al. (1987) for a longer time-series of cavate cysts. The data for this Jurassic-Pleistocene time-series show a much larger increase in mean endocyst size and EN:EC ratios for cavate cysts than is found in chorate cysts during the 'hothouse' interval from the upper Jurassic to Pliocene, followed by a very rapid decrease in both parameters for the cavate cysts. In contrast, the mean body size of all morphotypes and the EN:EC ratio in chorate cysts do not change much over the same time.

We consider that the reduction in size of parachute-like ectophragms which create a drag effect to slow the sinking of cysts below the pycnocline in stratified waters of marginal seas may have triggered the explosive evolution of the extraordinary flattened cruciform shape. The cross shape orients a cyst horizontally like a mica clay flake, thereby increasing the cell form resistance and reducing the sinking rate by maximising the surface area relative to the cell volume. However, it is not a simple step to transform a spherical body to a cross shape. This process initially requires the transformation of a sphere to an ellipse, followed by down-warping of the sides and flattening to accommodate the equatorial stretching of the elliptical body (Figure 7A). Given the complexity of these transformations from a presumed basic gonyaulacaean proximate cyst (Figure 7B), it is surprising that the cruciform endocyst morphology appears to have arisen in two separate cyst lineages: 1) a camocavate lineage with a pterate structure formed by a ventral ectocyst 'pull-apart' mechanism analogous to (although not the same as) that in the fibrous circumcavate cribroperidinoid genera *Thalassiphora* and *Romanodinium*, and 2) a proximochorate/chorate gonyaulacoid lineage with membranous 'wing-like' flanges formed by wide septa linking the processes, sometime strengthened by trabeculae between the process tips.

Although incubation experiments with cyst production within the *Gonyaulax spinifera* 'complex' (Rochon et al. 2009) demonstrate that cyst morphology can vary from the typical proximochorate/chorate features of *Spiniferites ramosus* and *Spiniferites mirabilis* to either the complex trabeculate characteristics of *Nematosphaeropsis labyrinthus* or the extreme proximate form of *Tectatodinium pellitum* Wall 1967 emend. Head 1994 with complex tegillate wall structure, none of the morphotypes displayed camocavate body wall development. This suggests that the proximochorate and cavate cyst developments are highly conservative features not subject to the greater plasticity of process length and wall surface texture. Likewise, Ellegaard (2000) has shown morphological variation in process length and endocyst shape (from spherical to ovate) occurs in cultures of *Spiniferite*s species subject to variable salinity but there was no production of a cruciform endocyst shape. In another experiment, Logares et al. (2007)

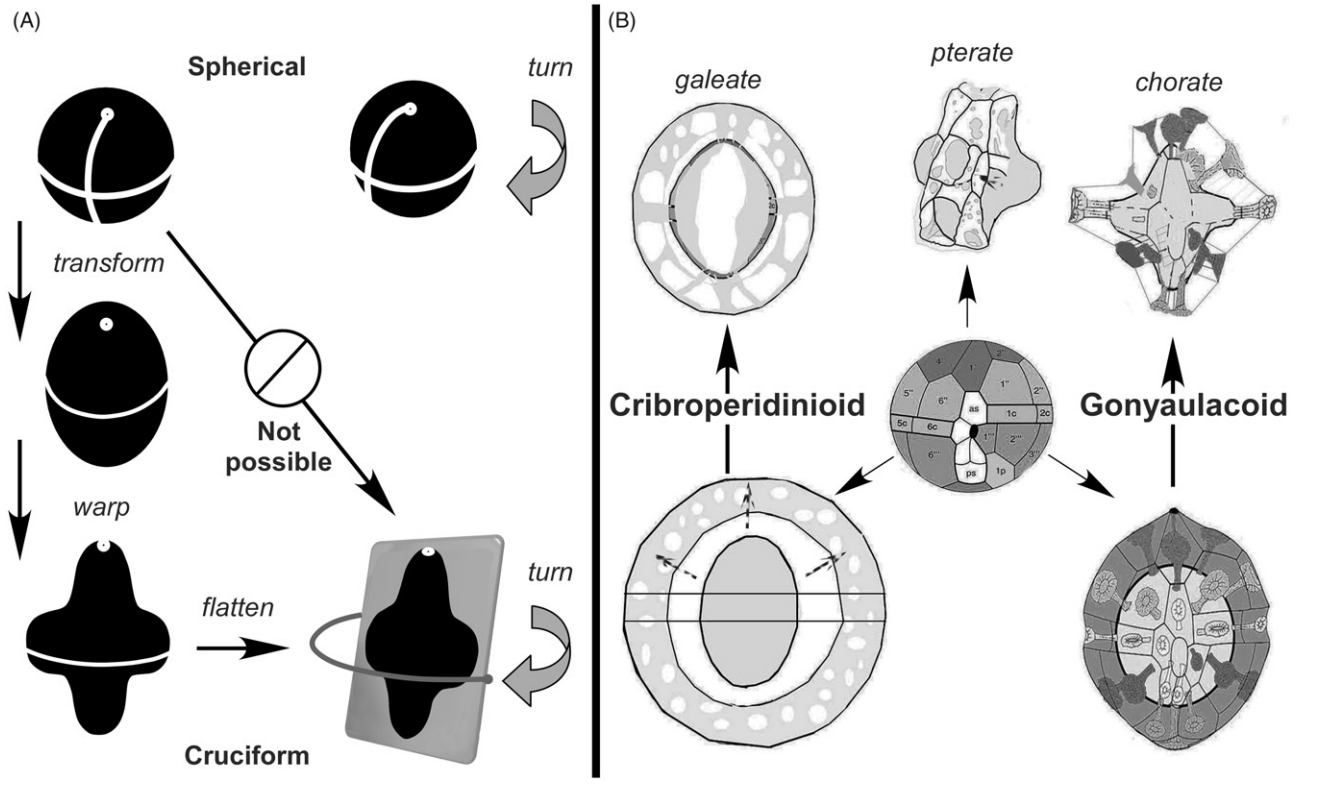

Figure 7. Sketches demonstrating most likely pathways of cruciform cyst evolution from a presumed spherical proximate cyst. A. Geometry of the transformation from sphere to cross-shape which is impossible to occur in one step but requires elongation, followed by warping and flattening. Curved arrows show lateral views of spherical vs. flattened cysts. 7B. Possible evolutionary pathways in the development of camocavate and chorate cruciform cysts from a presumed proximate gonyaulacacean ancestor with typical paratabulation (tabulated proximate cyst and pull-apart chorate images are from Fensome et al. 1993). All images depict ventral views.

showed that variable salinity influences the development of processes and amounts (cell densities ml^{-1}) of deformed specimens in cultures of the Baltic species *Scrippsiella hangoei* (Schiller 1935) Larsen 1995 and lake species *Peridinium aciculiferum* Lemmermann 1900 but there was no change in fundamental endocyst shapes (ovoid and elliptical, respectively), again suggesting that this is a highly conservative feature. In the Black Sea, however, the variation in the shape of the proximate cyst *Pyxidinopsis psilata* (*Tectatodinium psilatum* of Wall et al. 1973) displays an extraordinarily wide range in shape from spherical to strongly cruciform (Mudie et al. 2017, and Rochon, unpublished data).

Given that most taxa in the '*Gonyaulax etrusca* complex' may still be extant in the marginal easternmost area of their formerly widespread distribution, one would like to see the cysts grown in culture to determine their motile affinities, and their rDNA profiles should reveal the genetic relationships among the members. Unfortunately, so far, repeated efforts to grow the most widespread and abundant species *Spiniferites cruciformis* have failed either to survive in culture or immediately after germination which was followed by the rapid death and deterioration of the excysted motile cell (Kenneth Mertens, personal communication, 2015). Therefore we must now rely on our morphological studies of fossil cysts to assess the likelihood of a single evolutionary series as proposed by Popescu et al. (2009) versus two or three convergent lineages as proposed in this paper (Figure 7B).

5. Conclusions

The precise term cruciform originally used in 1973 to describe the endocyst outline of the proximochorate species *Spiniferites cruciformis* gradually has been broadened to include rhombiform-subpentagonal, elliptical, and other cyst body shapes in camocavate-circumcavate taxa so that its original precise meaning to describe a flattened, cross-shaped cyst is effectively becoming lost. More precise definition of galeate and pterate pericyst forms in the camocavate species *Galeacysta etrusca* and *Pterocysta cruciformis* helps in the correct identification of these taxa and in distinguishing them from *Spiniferites cruciformis*. Although extreme reduction of processes in ecomorphotypes of *Spiniferites cruciformis* forms 4 and 5 makes identification of poorly preserved specimens difficult, it is possible to distinguish this species from the invariably cruciform endocysts of *Pterocysta cruciformis* by presence of vestigial paracingular and sulcal ornament on the ventral surface. These features are absent on the ventral and dorsal surfaces of the subpentagonal-rhomboidal species *Galeacysta etrusca* with reduced periphragm development. In this camocavate species, raised or low septate paracingular ridges remain a distinguishing characteristic when the characteristic, dorso-laterally attached claustrate galea is reduced. Therefore, although EN:EC ratios may suggest a continuum of morphology in the '*Galeacysta etrusca* complex', this is a biometrical artefact that obscures the criteria differentiating the taxa and reduces the usefulness of separating the taxa for palaeoecological and chronostratigraphic studies. Cruciform endocyst shape appears to have evolved separately in the proximochorate genus *Spiniferites* and the camocavate genus *Pterocysta,* possibly in response to Plio-Pleistocene cooling and the need to conserve growth energy in marginal seas subject to extreme variations in salinity.

New distribution data on the occurrences of the taxa in modern and Holocene sediments of the Ponto-Caspian Seas and neighbouring lakes show that only chorate morphotypes of *Spiniferites cruciformis* are common throughout the region today, although cysts with reduced ornament (but not proximate forms) may co-occur in low amounts in the southern Caspian Sea. Morphotypes of *Spiniferites cruciformis* with pyriform endocysts are essentially confined to the endorheic seas where salt composition differs greatly from normal seawater in which NaCl is the dominant salt. Sparse amounts of *Galeacysta etrusca* and *Pterocysta cruciformis* are reported for Holocene sediments of the Caspian and Aral Seas but recent occurrences are only confirmed for the lowest salinity sector of our study region, in the Volga Delta area of the northern Caspian Sea where the three taxa may co-exist as cold-tolerant relicts of the once-extensive temperate Paratethyan Sea. Limited chrono stratigraphic data suggest there is a replacement of large Palaeogene marine-brackish water camocavate-circumcavate taxa with elliptical endocysts by the large Miocene rhombo-subpentagonal galeate species *Galeacysta etrusca* and then by the smaller Pliocene – Holocene semi-marine – brackish cruciform species *Spiniferites cruciformis* and stenohaline *Pterocysta cruciformis*.

Acknowledgements

Kenneth Mertens (while at Ghent University) is thanked for his loan of a slide from the Maccarone section and multiple discussions over several years. We also thank Adele (University of Florence) and Suzanne Leroy (Brunel University) for LM images, and Francesca Sangiorgi (Utrecht University) for loan of a slide from a Taman Peninsula section. Arjen Grothe (Utrecht University), Speranta M. Popescu (GeoBioStrat Consulting), and RA Fensome at Geological Survey of Canada Atlantic contributed several images and provided invaluable discussion and advice, as did Lucy Edwards (U.S.Geological Survey) who was one of two reviewers. Some of the results presented in this paper (including Figure 5) are part of Shannon Ferguson's Master Thesis project, under the direction of Sophie Warny and S-M. Popescu) and thanks are extended to Gilles Escarguel (Lyon, France) for the statistical analysis of Ferguson's data. Thanks to Ali Aksu and Helen Gillespie, Memorial University of Newfoundland for samples and lab processing, respectively. KR acknowledges the assistance of Jonah Chitolie (Geo-Techniques Research, UK) and Malcolm Jones (PLS Ltd., UK) for slide preparations, Delft University of Technology, The Netherlands, for providing the Emba Delta samples, CASP (Cambridge, UK) for providing the outcrop samples from Azerbaijan, and Moscow State University, Faculty of Geography, for allowing access to samples from the Volga Delta.

Funding

Shannon Ferguson's MSc thesis was funded by the Louisiana State University Museum of Natural Science and by the LSU Department of Geology and Geophysics. AR research is funded by NSERC Discovery Grant Program no. 05609; much of PM research was supported by NSERC Discovery Grant Program no. 206522 awarded while Adjunct Professor at MUN. This is ESS Contribution no. 20160016 of NRCan.

References

Aksu AE, Hiscott RN, Kaminski MA, Mudie PJ, Gillespie H, Abrajano T, Yaşar, D. 2002. Last glacial - Holocene paleoceanography of the Black Sea and Marmara Sea: stable isotopic, foraminiferal and coccolith evidence. Mar Geol. 190:119–149.

Bakrač K, Koch G, Sremac J. 2012. Middle and Late Miocene palynological biozonation of the south-western part of Central Paratethys (Croatia). Geol Croatica. 65:207–222.

Balteş N. 1971. Pliocene dinoflagellata and acritarcha in Romania. Proc. II Planktonic Conference Roma 1970, v.1:1 – 11.

Benedek PN, Gocht H. 1981. Thalassiphora pelagica (Dinoflagellata, Tertiär): electron-mikroskopische untersuchung und gedanken zur paläobiologie. Paleontogr Abt B. 180: 39–64.

Bertini A. 1992. Palinologia ed aspetti ambientali del versante adriatico dell'Appennino centro-settentrionale durante il Messiniano e lo Zancleano [Unpublished PhD Dissertation]. Italy: University of Modena. 88 p.

Bertini A. 2006. The Northern Apennines palynological record as a contribute for the reconstruction of the Messinian palaeoenvironments. Sed Geol. 188–189: 235–258.

Bertini A, Corradini, D. 1998. Biostratigraphic and paleoecological significance of *Galeacysta etrusca* in the 'Lago-mare' facies from the Mediterranean area (Neogene). Dino 6, NTNU Vitenskapsmuseet Rappot botanisk Serie 1998. Abstract, p. 15–16.

Bertini A, Corradini D, Suc P. 1995. On *Galeacysta etrusca* and the connections between the Mediterranean and the Paratethys. Sed Geol Rom J Strat. 76:141–142.

Bradley LR, Marret F, Mudie PJ, Aksu AE, Hiscott R. 2013. Constraining Holocene sea-surface conditions in the south-western Black Sea using dinoflagellate cysts. J Quat Sci. 27: 835–843.

Cohen KM, Finney S, Gibbard, PL, Fan J.-X. 2013; updated. The ICS International Chronostratigraphic Chart. Episodes 36: 199 – 204. Also accessible at http://www.stratigraphy.org/ICSchart/ChronostratChart2016-04.pdf.

Corradini D, Biffi U. 1988. Dinocyst study at the Messinian-Pliocene boundary in the Cava Serridi section, Tuscany, Italy. Bull Centres Rech Explor-Prod Elf-Aquitaine. 12:221–236.

Cosentino D, Bertini A, Cipollari P, Florindo F, Gliozzi E, Grossi F, Lo Mastro S, Sprovieri, M. 2012. Orbitally forced paleoenvironmental and paleoclimate changes in the late postevaporitic Messinian of the central Mediterranean Basin. Geol Soc Am Bull. 124:499–516.

Dale B. 1996. Dinoflagellate cyst ecology: modeling and geological applications. In: Jansonius J, McGregor DC (editors). Palynology: Principles and Applications. Dallas, Texas: American Association of Stratigraphic Palynolologists Foundation. Vol. 3; p. 1249–1276.

de Verteuil L, Norris G. 1996. Miocene dinoflagellate stratigraphy and systematics of Maryland and Virginia. Micropaleontology. 42(suppl), 1–172.

Do Couto D, Popescu S-M, Suc J-P, Melinte-Dobrinescu MC, Barhoun N, Gorini C, Jolivet L, Poort J, Jouannic G, Auxietre J-L et al. 2014. Lago Mare and the Messinian Salinity Crisis: Evidence from the Alboran Sea (S. Spain). Mar Petrol Geol. 52:57–76.

Eaton GL. 1975-1976. Dinoflagellate cysts from the Bracklesham beds Eocene of the Isle of Wight Southern England. Bull Brit Mus. (Nat Hist.) 26:284–289.

Eaton GL. 1996. *Seriliodinium*, a new Late Cenozoic dinoflagellate cyst. Rev Paleobot Palynol. 91:151–1689.

Ellegaard M. 2000. Variations in dinoflagellate cyst morphology under conditions of changing salinity during the past 2000 years. Rev Palaeobot Palynol. 109:65–81.

Fensome RA, Williams GL. 2004. Scotian Margin PalyAtlas. Version 1. Dartmouth (NS): Geological Survey of Canada. Open File 4677.

Fensome RA, Taylor FJR, Norris G, Sarjeant QAS, Wharton DI, Williams GL. 1993. A classification of living and fossil dinoflagellates. Micropaleo. Spec Publ. 7:1–351.

Ferguson S, 2012. Evaluation of Pleistocene to Holocene (MIS 5 to 1) climatic changes in southwestern Black Sea: a palynological study of DSDP Site 380A [MSc dissertation]. Baton Rouge: Department of Geology and Geophysics, Lousiana State University; 64 p; http://etd.lsu.edu/docs/available/etd-04172012-223524/unrestricted/ShannonFergusonThesis.pdf.

Ferguson S, Warny S, Escarguel G, Mudie P. 2018. MIS 5 to 1 dinoflagellate cyst analyses analyses and morphometric evaluation of Galeacysta etrusca and Spiniferites cruciformis in southwestern Black Sea. Quat Internat. 465:117–129.

Grothe A, Sangiorgi F, Mulders YR, Vasiliev I, Reichart G-J, Brinkhuis H. 2014. Black Sea desiccation during the Messinian salinity crisis: fact or fiction? Geology. 42:563–566.

Haghani S, Leroy SAG, Khdir S, Kabiri K, Beni KN, Lahijani, HAK. 2015. An early 'Little Ice Age' brackish water invasion along the south coast of the Caspian Sea (sediment of Langarud wetland) and its wider impacts on environment and people. The Holocene. 26:3–16.

Jimenez-Moreno G, Head MJ, Harzhauser M. 2006. Early and Middle Miocene dinoflagellate cyst stratigraphy of the Central Paratethys, Central Europe. J Micropalaeo. 25:113–139.

Kazancı N, Gulbabazadeh T, Leroy SAG, Ileri, Ö. 2004. Sedimentary and environmental characteristics of the Gilan-Mazenderan plain, northern Iran: influence of long- and short-term Caspian water level fluctuations on geomorphology. J Mar Syst. 46:145–168.

Kloosterboere-van Hoeve ML, Steenbrink J, Brinkhuis H. 2001. A short-term cooling event 4.205 million years ago, in the Ptolemais Basin, Northern Greece. Palaeogeog, Palaeoclimat, Palaeoecol. 173:61–73.

Kontopoulos N, Zelilidis A, Piper DJW, Mudie PJ. 1997. Messinian evaporites at Zakynthos, Greece. Palaeogeog, Palaeoclim, Palaeoecol. 129:361–367.

Kosarev AN, Yablonskaya EA. 1994. The Caspian Sea. The Hague, The Netherlands: SPB Academic Publishing, 259 p.

Kouli K, Brinkhuis H, Dale B. 2001. *Spiniferites cruciformis*: A Fresh Water Dinoflagellate Cyst? Rev Palaeobot Palynol. 113:273–286.

Leroy SAG. 2010. Palaeoenvironmental and palaeoclimatic changes in the Caspian Sea region since the Lateglacial from palynological analyses of marine sediment cores. Geog, Environ, Sustain. 3:14–32.

Leroy SAG, Albay M. 2010. Palynomorphs of brackish and marine species in cores from the freshwater Lake Sapanca, NW Turkey. Rev Palaeobot Palynol. 160:181–188.

Leroy SAG, Marret F, Gilbert E, Reyss, Jll, Arpe K. 2007. River inflow and salinity changes in the Caspian Sea during the last 5500 years. Quat Sci Rev. 26:3359–3383.

Leroy SAG, Tudryn A, Chalié F, López-Merino L, Gasse F. 2013. From the Allerød to the mid-Holocene: palynological evidence from the south basin of the Caspian Sea. Quat Sci Rev. 78:77–97.

Leroy SAG, López-Merino L, Tudryn A, Chalié F, Gasse F. 2014. Late Pleistocene and Holocene palaeoenvironments in and around the Middle Caspian Basin as reconstructed from a deep-sea core. Quat Sci Rev. 101:91–110.

Lewis SL, Maslin MA. 2015. Defining the Anthropocene. Nature. 5 – 9:171–180.

Logares R, Rengefors K, Kremp A, Shalchian-Tabrizi K, Boltovskoy A, Tengs T, Shurtleff A, Klaveness D. 2007. Phenotypically different microalgal morphospecies with identical ribosomal DNA: a case of rapid adaptive evolution? Microb Ecol. 53:549–561.

Londeix L, Benzakour M, Suc J-P. 2007. Messinian palaeoenvironments and hydrology in Sicily (Italy): The dinoflagellate cyst record. Geobios. 40:233–250.

Londeix L, Herreyre Y, Turon J-L, Fletcher, W. 2009. Last glacial to Holocene hydrology of the Marmara Sea inferred from a dinoflagellate cyst record. Rev Palaeobot Palynol. 158:52–71.

Magyar I, Geary DH, Muller P. 1999. Paleogeographic evolution of the Late Miocene Lake Pannon in Central Europe. Palaeogeog Palaeoclim Palaeoecol. 147:151–187.

Marret F, Leroy S, Chalié F, Gasse F. 2004. New organic-walled dinoflagellate cysts from recent sediments of Central Asia: Rev Palaeobot Palynol. 129:1–20.

Matenco L, Munteanu I, ter Borgh M, Stanica A, Tilita M, Lericolais G, Dinu C, Oaie G. 2016. The interplay between tectonics, sediment dynamics and gateways evolution in the Danube system from the Pannonian Basin to the western Black Sea. Sci Total Environ. 543:807–827.

Mertens KN, Bradley LR, Takano Y, Mudie PJ, Marret F, Aksu AE, Hiscott RN, Verleye TJ, Mousing EA, Smyrnova LL. 2012. Quantitative estimation of Holocene surface salinity variation in the Black Sea using dinoflagellate cyst process length. Quat Sci Rev. 39:45–59.

Mudie PJ, Asku AE, Yasar D. 2001. Late Quaternary dinoflagellate cysts from the Black, Marmara and Aegean seas: variations in assemblages, morphology and paleosalinity. Mar Micropaleo. 43:155–178.

Mudie PJ, Marret F, Mertens KN, Shumilovskikh L, Leroy SAG. 2017. Atlas of modern dinoflagellate cyst distributions in the Black Sea Corridor: from Aegean to Aral Seas, including Marmara, Black, Azov and Caspian Seas. Mar Micropalentol. 134:1–152.

Mudie PJ, Rochon A, Aksu AE, Gillespie H. 2002. Dinoflagellate cysts, freshwater algae and fungal spores as salinity indicators in Late Quaternary cores from Marmara and Black Seas. Mar Geol. 190:203–231.

Mudie PJ, Rochon A, Aksu AE, Gillespie H. 2004. Late glacial, Holocene and modern dinoflagellate cyst assemblages in the Aegean-Marmara-Black Sea corridor: statistical analysis and re-interpretation of the early Holocene Noah's Flood hypothesis. Rev Palaeobot Palynol. 128:143–167.

Norris G. 1978. Phylogeny and a revised super-generic classification for Triassic-Quaternary organic-walled dinoflagellate cysts (Pyrrhophyta). Part II. Families and sub-orders of fossil dinoflagellates. Neues Jahrb Geol Paläont. 156:1–30.

Piller WE, Mathias Harzhauser M, Mandic O. 2007. Miocene Central Paratethys stratigraphy – current status and future directions. Stratigraphy. 4:151–168.

Popescu S-M, Melinte M-C, Suc J-P, Clauzon G, Quillévéré F, Süto-Szentai M. 2007. Earliest Zanclean age for the Colombacci and uppermost Di Tetto formations of the ''latest Messinian'' northern Apennines: new palaeoenvironmental data from the Maccarone section (Marche Province, Italy). Geobios. 40:359–373.

Popescu S-M, Dalesme F, Escarguel G, Head MJ, Melinte-Dobrinescu MC, Süto-Szentai M, Bakrač K, Clauzon G, Suc J-P. 2009. *Galaecysta etrusca* complex: dinoflagellate cyst marker of Paratethyan influxes to the Mediterranean Sea before and after the peak of the Messinian salinity crisis. Palynology. 33: 105–134.

Popescu S-M, Dalibard M, Suc J-P, Barhoun N, Melinte-Dobrinescu M-C, Bassetti MA, Deaconu F, Head MJ, Gorini C, Do Couto D, et al. 2015. Lago Mare episodes around the Messinian-Zanclean boundary in the deep southwestern Mediterranean. Mar Petrol Geol. 66:55–70.

Richards K. 2012. Palynology, vegetation and climate of latest Miocene, Pliocene and early Pleistocene sediments of the Caspian Sea: a detailed study of several outcrop localities in Azerbaijan. Abstract. 13th International Palynological Congress, Tokyo, Japan, 23-30 August 2012. In: Japanese Journal of Palynology, no 58; Special Issue Abstracts IPC/IOPC 2012, p. 195 – 196.

Richards K, Leroy SAG, Arpe K, Marret F, Hoogendoorn RM, Kroonenberg SB. 2011. Fluctuations in Caspian Sea Level during the Quaternary: new evidence from palynology, ostracods and climate modeling. Extended abstract. 3rd International Symposium on the Geology of the Black Sea region, Bucharest, Romania, 1-10 October 2011; In: Abstracts, Supplement to Geo-Eco-Marina, no. 17: p. 144 – 147.

Richards K, Bolikhovskaya NS, Hoogendoorn RM, Kroonenberg SB, Leroy SAG, Athersuch J. 2014a. Reconstructions of deltaic environments from Holocene palynological records in the Volga delta, northern Caspian Sea. The Holocene. 24:1226–1252.

Richards K, Athersuch J, Hoogendoorn RM, van Baak CGC, Wonders, AAH. 2014b. New palynological and microfossil studies of Pleistocene outcrops (Akchagyl) and core samples (Apsheronian, Bakunian, Khazarian and Khvalynian) in the western, central and northeastern Caspian Sea region. Extended abstract. IGCP 610 Second Plenary Meeting and Field Trip, Baku, Azerbaijan, 12-20 October 2014. In: Stratigraphy and sedimentology of oil-gas basins (Special Issue); Azerbaijan National Academy of Sciences, p. 117 – 119.

Roberts K. 2012. Paleoenvironment of Marmara Sea: Palynology of Upper Pleistocene-Holocene sediments in long piston cores [MSc Dissertation]. Canada: Department of Earth Sciences, Memorial University of Newfoundland, 160 p.

Rochon A, Mudie PJ, Aksu A.E, Gillespie H. 2003. *Pterocysta* gen. nov.: a new dinoflagellate cyst from Pleistocene glacial-stage sediments of the Black and Marmara seas. Palynology. 26:95–105.

Rochon A, Lewis J, Ellegaard M, Harding IC. 2009. The *Gonyaulax spinifera* (Dinophyceae) 'complex': Perpetuating the paradox? Rev Palaeobot Palynol. 155:52–60.

Sarjeant WAS. 1974. Fossil and living dinoflagellates. London: Academic Press Inc.

Sarjeant WAS, Lacalli T, Gaines G. 1987. The cysts and skeletal elements of dinoflagellates: speculations on the ecological causes for their morphology and development. Micropaleo. 33:1–36.

Servais T, Eiserhardt, KH. 1995. A discussion and proposals concerning the lower paleozoic "galeate" acritarch plexus. Palynology. 19:191–210.

Shumilovskikh LS, Marret F, Fleitmann D, Arz HW, Nowaczyk N, Behling H. 2013. Eemian and Holocene sea surface conditions in the southern Black Sea: organic-walled dinoflagellate cyst record from core 22-GC3. Mar Micropaleontol. 101:146–160.

Snel E, Mărunţeanu M, Macaleţ R, Meulenkamp JE, van Vugt N. 2006. Late Miocene to Early Pliocene chronostratigraphic framework for the Dacic Basin, Romania. Palaeogeog, Palaeoclimatol, Palaeoecol. 238:107–124.

Sorrel P, Popescu, S.-M, Head MJ, Suc JP, Klotz S, Oberhänsli H. 2006. Hydrographic development of the Aral Sea during the last 2000 years based on a quantitative analysis of dinoflagellate cysts. Palaeogeog, Palaeoclimat, Palaeoecol. 234:304–327.

Stoffers P, Degens ET, Trimonis, ES. 1978. Stratigraphy and suggested ages of Black Sea sediments cored during Leg. 42B. In: Ross DA, Neprochnov YP, et al., (editors). Initial Reports of the Deep Sea Drilling Project. Washington: U.S. Government Printing Office; Vol. 42; p. 483–488.

Stover LE, Evitt WR. 1978. Analyses of pre-Pleistocene organic-walled dinoflagellates. Stanford University publications, Geological sciences. Vol. 15, 300 p.

Suc J-P, Gillet H, Çağatay MN, Popescu S-P, Lericolais G., Armijo R, Melinte-Dobrinescu, MC, Şevket Ş, Clauzon, G., Sakinç M. et al. 2015. The region of the Strandja Sill (North Turkey) and the Messinian events. Mar Petrol Geol. 66:149–164.

Sütő-Szentai M. 1986. A magyarországi Pannoniai (s.l.) rétegösszlet mikroplankton vizsgálata. Folia Comloensis. 2:25–45.

Sütő-Szentai M. 1988. Microplankton zones of organic skeleton in the Pannonian *s.l.* stratum complex and in the upper part of the Sarmatian strata. Acta Botan Hungarica. 34:339–356.

Sütő-Szentai M. 1990. Mikroplanktonflora der pontischen (oberpannonischen) Bildungen Ungarns. Pliozän Pt. I, Pontien. In: Stevanović P (editor). Chronostratigraphie und Neostratotypen, Pliozän Pt. I, Pontien, p.842–869; Yugoslavia: JAZU and SANU, Zagreb and Belgrade.

Sütő-Szentai M. 2000. Organic walled microplankton zonation of the Pannonian s.l. in the surroundings of Kaskantyu, Paks and Tengelic (Hungary). Ann Rept Geol Inst Hungary, 1994–1995/II:153–175.

Sütőné Szentai M. 1989. A Szentlőrinc-XII. sz. Szerkezetkutató fúrás pannóniai rétegsorának szervesvázú mikróplankton flórája. Foldtani Kozlony, Bull Hungar Geol Soc. 119:31–43.

Sütőné Szentai M. 2010. Definition and description of new dinoflagellate genus, species and subspecies from the Pannonian Stage (Hungary). Acta Nat Pannon. 1:223–239.

Sütőné Szentai M, Ildikó S. 2003. Felszí also Pannóniai elöfordulás felcsúton szervesvázú mikroplankton és sporomorpha maradványok. Folio Musei Hostorico-Naturalist Bakonyiensis a Bakonyi Természettudományi Múzeum Közleményei Zirc 20:47–62 (in Hungarian).

Sütő Zoltánné M. 1994. Microplankton associations of organic skeleton in the surroundings of Villany Mts. Földtani Közlöny. 124:451–478.

van Baak CGC. 2015. Mediterranean-Paratethys connectivity during the late Miocene to Recent: unravelling geodynamic and paleoclimatic causes of sea-level change in semi-isolated basins. [Unpublished PhD thesis], University of Utrecht, The Netherlands. Utrecht Studies in Earth Sciences, 87: 275 p.

Versteegh GJM, Zevenboom D. 1995. New genera and species of dinoflagellate cysts from the Mediterranean Neogene. Rev Palaeobot Palynol. 85:213–229.

Wall D, Dale B, Harada K. 1973. Descriptions of new fossil dinoflagellates from the late Quaternary of the Black Sea. Micropaleo. 19:18–31.

Warny S, Wrenn JH. 1997. New species of dinoflagellate cysts from the Miocene-Pliocene boundary on the Atlantic coast of Morocco. Rev Paleobot Palynol. 96: 281–304.

Warny S, Wrenn JH. 2002. Upper Neogene dinoflagellate cyst ecostratigraphy of the Atlantic coast of Morocco. Micropaleontology. 48: 257–272.

Warny S, Bart PJ, Suc JP. 2003. Timing and progression of climatic, tectonic and glacioeustatic influences on the Messinian Salinity Crisis. Palaeogeog, Palaeoclim, Palaeoecol. 202:59–66.

Williams GL, Fensome RAF, Miller MA, Sarjeant WAS. 2000. A glossary of the terminology applied to dinoflagellates, acritarchs and prasinophytes, with emphasis on fossils. 3rd ed. Dallas (TX): AASP Contributions Series Number 37, AASP Foundation, 281 p.

Zenkevitch L. 1963. Biology of the Seas of the U.S.S.R. London: Interscience Publishers and George Allen and Unwin Ltd.